uOttawa

L'Université canadienne
Canada's university

FACULTÉ DES ÉTUDES SUPÉRIEURES ET POSTOCTORALES

uOttawa

L'Université canadienne
Canada's university

FACULTY OF GRADUATE AND POSDOCTORAL STUDIES

Lunde Huang

AUTEUR DE LA THÈSE / AUTHOR OF THESIS

M.Sc. (Cellular and Molecular Medicine)

GRADE / DEGREE

Department of Cellular and Molecular Medicine

FACULTÉ, ÉCOLE, DÉPARTEMENT / FACULTY, SCHOOL, DEPARTMENT

Identification and Classification of *JIGR1*,
A Novel MADF-Containing Gene Essential for *Drosophila* Development

TITRE DE LA THÈSE / TITLE OF THESIS

Dr. M. Sonnenfeld

DIRECTEUR (DIRECTRICE) DE LA THÈSE / THESIS SUPERVISOR

CO-DIRECTEUR (CO-DIRECTRICE) DE LA THÈSE / THESIS CO-SUPERVISOR

EXAMINATEURS (EXAMINATRICES) DE LA THÈSE / THESIS EXAMINERS

Dr. K. Turksen

Dr. M. Ekker

Gary W. Slater

Le Doyen de la Faculté des études supérieures et postdoctorales / Dean of the Faculty of Graduate and Postdoctoral Studies

Identification and Classification of *JIGR1*, A Novel MADF-Containing Gene Essential for *Drosophila* Development

Lunde Huang

This thesis is submitted as a partial fulfillment of
The M.Sc. program in Cellular and Molecular Medicine

Department of Cellular and Molecular Medicine
Faculty of Medicine
University of Ottawa

May 2008

Your file Votre référence
ISBN: 978-0-494-48464-7
Our file Notre référence
ISBN: 978-0-494-48464-7

ACKNOWLEDGEMENTS

I would like to give my most heartfelt thanks to Dr. Margaret Sonnenfeld for everything she has done for me. Her love and enthusiasm for research is truly infectious and inspiring. Most of all, I am grateful for her guidance, patience and terrific friendship. My deepest gratitude to Xuetao Sun, whose attitude and passion for science and life I will always admire and strive for. I cannot imagine completing this without the countless hours he has spent answering my questions and assisting me every step of the way. I would like to sincerely thank Tatiana Morozova and M'omena Dawood for their generosity and wonderful company. I consider myself incredibly lucky to have been a part of the Sonnenfeld lab, where laughter is a requisite and the flies are our 'babies'.

A very special thanks to the many students and staff of CMM and NSC who have graciously allowed me to borrow, probe, and inquire; but above all, given me friendships I will treasure forever.

I would also like to thank the members of my committee, Dr. Marc Ekker and Dr. Christine Pratt for their time, input and assistance.

Lastly, I would like to thank my family for their endless support and love.

ABSTRACT

The *Drosophila melanogaster* model system is capable of providing valuable insight to neurodegenerative disease research. The *Drosophila jing* zinc finger transcription factor plays an essential role in CNS and tracheal cell differentiation. It is important to identify and characterize *jing* interactors to better understand its molecular mechanism. The *JIGR1* gene was previously identified as a genetic modifier of *jing* and contains a MADF DNA-binding domain. The MADF domain is found in a large and diverse family with weak sequence homology. *JIGR1* was found to genetically interact with other *jing*-interactors to maintain photoreceptor survival. JIGR1 is predominantly localized to the nuclei and is ubiquitously present throughout all stages of embryogenesis, particularly in the CNS and PNS, suggesting a role in fundamental cellular processes. Proper regulation of JIGR1 dosage is important, as its over-expression is associated with defects in the CNS and tracheal development. By characterizing *JIGR1* and having a better concept of *jing*, with a homolog found in vertebrates, a better understanding of the complex vertebrate developmental pathways is gained.

TABLE OF CONTENTS

LIST OF FIGURES

LIST OF ABBREVIATIONS

aa	amino acids
AB_{1-42}	amyloid-$ß_{1-42}$
AC	anterior commissure
AD	Alzheimer's disease
Adf-1	alcohol dehydrogenase transcription factor 1
AEL	after egg laying
APP	amyloid precursor protein
BDGP	Berkeley Drosophila Genome Project
BHLH-PAS	basic-helix-loop-helix-PAS
BLAST	Basic Local Alignment and Search Tool
bnl	*branchless*
btl	*breathless*
C/EBP	CCAAT enhancer binding protein
CME	central midline elements
CNS	central nervous system
comm	*commissureless*
DA	dopaminergic
DATR-X	Drosophila α-thalassemia/mental retardation X-linked
Dip3	Dorsal-interacting protein 3
EGFR	epidermal growth factor receptor
EMS	ethyl methane sulphonate
EP	enhancer/promoter
FGFR	fibroblast growth factor receptor
fra	*frazzled*
ftz	*fushi tarazu*
gcm	*glial cell missing*
gmr	*glass multiple reporter*
GOF	gain-of-functios
GST	Glutathione-S-transferase

HA	hemagglutinin
JIGR1	*jing-interacting regulatory gene-1*
JNK	Jun-N-terminal kinase
LC	longitudinal connectives
LM	light microscopy
LRR	leucine-rich repeat
MADF	Myb/SANT-like domain in Adf-1
MG	midline glia
NB	neuroblasts
net	*netrin*
NLS	nuclear localization sequence
PC	posterior commissure
PD	Parkinson's disesease
PNS	peripheral nervous system
prd	*paired*
pros	*prospero*
rho	*rhomboid*
robo	*roundabout*
RT	room temperature
SEM	Scanning Electron Microscope
sim	*single-minded*
slbo	*slow border cell*
slt	*slit*
spry	*sprouty*
SMART	Simple Modular Architecture Research Tool
SRF	serum response factor
trh	*trachealess*
tgo	*tango*
UAS	Upstream Activation Sequence
VNC	ventral nerve cord
vvl	*ventral veins lacking*

INTRODUCTION

1.1 A Model Organism

Not surprisingly, one of the most popular animal models employed in biology today is the *Drosophila melanogaster*. This little fruit fly, though seemingly simple in structure, contains a wealth of advantageous characters and abundant genetic markers. The utilization of *Drosophila* as a model organism has come a long way since it was first employed by Thomas Hunt Morgan to demonstrate chromosomes as the mechanical basis of Mendelian inheritance in the early 1900's. Along with the sequencing of its entire genome, protein null loss-of-function mutations are available for several thousand genes, rendering it a highly desirable molecular tool. Originally used most often in genetic studies, scientists have since discovered that the simple fruit fly can be used extensively in numerous fields of biology, from behavioural biology to neuropharmacological research (Manev *et al.*, 2003). The utility of *Drosophila* as a model organism for the study of human genetic disease is now well documented; one analysis identified 714 distinct human disease genes (77% of disease genes searched) have matches in 548 unique *Drosophila* sequences (Reiter *et al.*, 2001).

Although the fly model is still relatively new to neurodegenerative disease research, it is quickly becoming a favourite to elucidate invaluable cellular and molecular mechanisms in many human neurodegenerative diseases (Chan and Bonini, 2000). The extensive homology of the human and *Drosophila* genomes forms the basis for ongoing loss-of-function studies, three quarters of the approximate 100 genes implicated in specific human diseases have at least one homolog in *Drosophila* (Sang and Jackson, 2005). Aside from the genes being highly conserved, the *Drosophila* central nervous system (CNS) is built from neurons and glia that operate on the same fundamental

principles as their mammalian counterparts (Shulman *et al.*, 2003), as well retains the ability to display complex behaviour such as learning and memory expected from more highly evolved organisms. With the assistance of powerful genetic tools, transgenic approaches have facilitated the development of *Drosophila* models that recapitulate key neuropathological features of Alzheimer's disease, Parkinson's disease, Huntington's disease, and several spinocerebellar ataxias allowing the identification and dissection of pathological pathways in the diseases (Shulman *et al.*, 2003;Crowther *et al.*, 2006).

1.1.1 Neurodegenerative diseases

Alzheimer's disease is classified by two major classic histopathologic features, the extracellular neuritic plaques (consisting of a central core of amyloid-$ß_{1-42}$ protein surrounded by astrocytes, microglia, and dystrophic neuritis) and the intracellular neurofibrillary tangles (composed of hyperphoshorylated tau protein that occupy the cell body and extend into the dendrites) (Cummings and Cole, 2002;Crowther *et al.*, 2006). In humans, the toxic peptide amyloid-$ß_{1-42}$ ($Aß_{1-42}$) accumulates due to cleavage mutations in the transmembrane protein amyloid precursor protein (APP) by ß- and γ-secretase. The *Drosophila* APP homolog, however, does not fully extend to the Aß portion of the protein, rendering *Drosophila* modeling of AD more challenging than other neurodegenerative diseases (Bilen and Bonini, 2005;Crowther *et al.*, 2006). An endogenous tau homologue is also present in flies, but directed over-expression of human tau is still preferred in models.

A triple transgenic fly co-expressing human APP, ß-secretase and fly γ-secretase has been created to faithfully reflect the processing of human APP with convincing phenotypes including formation of diffuse extracellular amyloid, impaired olfactory

associative learning and neurodegeneration in the retina (Sang and Jackson, 2005). Nevertheless, even non-transgenic flies composed strictly of *Drosophila APP-like* gene (dAPPL) have provided insight into various aspects of AD pathology. Over-expression of wild-type γ-secretase component, Presenilin, causes programmed cell death, providing evidence that cell loss mechanisms are associated with AD neurodegeneration (Bilen and Bonini, 2005). Similarly, deletion of dAPPL in larval motor neurons produces accumulation of organelles along axon tracts, which occurs upon loss of function of motor proteins and suggests that axonal disruption may play a role in the neurodegenerative pathology of AD (Gunawardena and Goldstein, 2001).

Parkinson's disease (PD) is an idiopathic disorder featuring resting tremor, rigidity, and bradykinesia, the slowness of voluntary movements. It is characterized by the loss of dopaminergic (DA) neurons in the midbrain and the accumulation of intraneuronal inclusions known as Lewy bodies that are composed of primary aggregated (fibrillar) α-synuclein (Volles and Lansbury, Jr., 2003;Sang and Jackson, 2005). Simple, monogenic forms of parkinsonism appear to be relatively rare, substantial evidence indicates that environmental factors and genetic factors both contribute to the etiology of PD. Even though the distribution of DA neurons in the CNS of *Drosophila* differs from that of vertebrate brains, the *Drosophila* genome encodes homologs of five of the six PD-related genes that have been identified (Whitworth *et al.*, 2006).

One of the first PD-related genes to be studied in the *Drosophila* is *α-synuclein*; although cases of dominant PD related to mutations in α-synuclein are extremely rare, it is a component of Lewy body inclusions and might provide more understanding of the underlying pathways resulting in the symptoms of PD (Polymeropoulos *et al.*, 1997). As

there appears to be no direct ortholog of the α-synuclein gene, transgenic flies expressing both normal and mutant human α-synuclein have been produced in hopes of modelling PD. Overall the nervous system is appropriately formed and the aging brain shows no widespread degenerative changes in α-synuclein transgenic flies; brain volume is likewise preserved in many patients with Parkinson's disease, but marked degeneration occurs in specific groups of neurons, such as DA (Feany and Bender, 2000). Analysis of the integrity of DA neurons in flies reveals that α-synuclein is cytotoxic causing a progressive loss of neuronal integrity and the presence of widespread cytoplasmic inclusion formation. A search of behavioural manifestations of nervous system dysfunction revealed that locomotor behaviour is grossly preserved in young flies, however, over time they decline in performance more rapidly than controls. The time course of locomotor dysfunction parallels the degeneration of dopaminergic neurons and the appearance of α-synuclein inclusions (Feany and Bender, 2000).

In the short time that *Drosophila* has been used for neurodegenerative disease research, fly models have proven to be a good place to start for discovering valuable insight into disease and identifying useful compounds. As techniques for analysis improve, *Drosophila* models will play important roles in the quest to develop cures for neurodegenerative disorders.

1.2 Embryonic Development of the CNS

Insects and vertebrates employ related molecules and mechanisms to construct basic structures of their nervous systems. It is therefore relevant to investigate this complex system made up of many distinct but interdependent developmental processes in

flies and beneficially apply it to higher organisms that are not as accessible to genetic analysis.

The CNS consists of two cell major cell types, the neurons and glial cells. These can be generated either by common precursors (neuroglioblasts) or by precursors that are specialized to produce either neurons (neuroblasts) or glial cells (glioblasts) (Egger *et al.*, 2002). The *Drosophila* CNS is composed of segments known as neuromeres which are formed from the ventral neuroepithelium after the gastrulation stage. Every neuromere can be divided into three major regions: the left and right neurogenic regions separated by a midline region. Neuromeres are bilaterally symmetrical in both the patterning of precursors and neurons as well as the innervation of peripheral tissues. The first-born neurons are found to be the closest to the inner surface of the developing neuroepithelium, and initiate growth cones that commence the formation of first axon pathways (pioneers). Within each neuromere, the axons develop in a scaffold patterning made up of a pair of bilaterally symmetrical longitudinal axon tracts with a pair of commissural axon tracts connecting the two sides in the middle, and a pair of nerve roots exiting the CNS on each side. Each major longitudinal tract is made up of 3 distinct axon bundles, or fascicles (Goodman and Doe, 1993).

1.2.1 Neurogenesis

a) **Neurogenic region:** The neurogenic region generates the bulk of the neurons in the CNS. It is designated by a strip of ventral ectoderm that contains specialized single cells which can develop into neural precursor cells called neuroblasts (NB). The transition of NB from ectoderm is both time and spatial specific (Figure 1) and requires that as these young NB enlarge they inhibit adjacent ectodermal cells from

becoming NB, a process known as lateral inhibition; adjacent cells then either differentiate into nonneuronal support cells or die (Doe and Goodman, 1985). Two classes of genes were discovered to regulate these processes:

(1) Proneural genes to control the time of NB formation

(2) Neurogenic genes to limit more than one group of cells from enlarging into NB

b) **Midline region:** A distinctive strip of midline cells separates the two neurogenic regions (Figure 1) and is responsible for generating a small number of special midline neurons and glial cells with various expression profiles (Goodman and Doe, 1993). Despite the small number of precursors found in the region, the midline neural epithelial cells play a key role in pathway guidance of axons (commissures) and longitudinal axons (Tessier-Lavigne *et al.*, 1988;Dickson and Gilestro, 2006).

Midline cells become molecularly specialized after the cellular blastoderm stage. This is characterized by the expression of the *single-minded* (*sim*) gene which is required in the development of the neurons, glia, and other nonneuronal cells that lie along the strip (Nambu *et al.*, 1990).

Previous work on putative CNS midline genes revealed the existence of central midline elements (CME), an enhancer element both required and sufficient for CNS midline transcription (Sonnenfeld *et al.*, 1997). There is direct evidence that Sim, a basic helix-loop-helix (bHLH)-PAS protein, dimerizes with fellow *Drosophila* bHLH-PAS protein Tango (Tgo), a broadly expressed protein homologous to mammalian ARNT (Sonnenfeld *et al.*, 1997). The two form a heterodimer that binds to CME, which in turn controls CNS midline transcription (Crews, 1998).

Figure 1. Development of the neurogenic region and ventral midline. Midline development occurs in four successive developmental stages (dorsal side up). During the first stage, blastoderm, mesectodermal cells or midline precursors are located on either side of the mesodermal anlage to separate the presumptive mesoderm from the presumptive neurogenic ectoderm. During gastrulation, the mesodermal cells invaginate and the mesectodermal cells meet at the ventral midline. As germ band elongation proceeds, these two rows of cells intermingle to form a row of midline precursor cells. In the final stage, along with the delaminating neuroblasts, the midline precursors must also delaminate before they divide to give rise to neurons and glial cells of the ventral midline. The transient gap is later filled in by rearrangement of epidermal cells. (Adapted from Goodman and Doe, 1993)

Cellular blastoderm

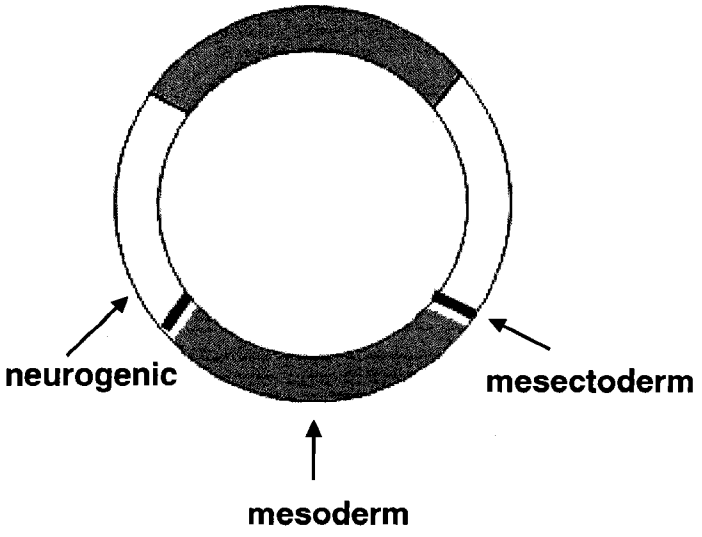

Gastrulation

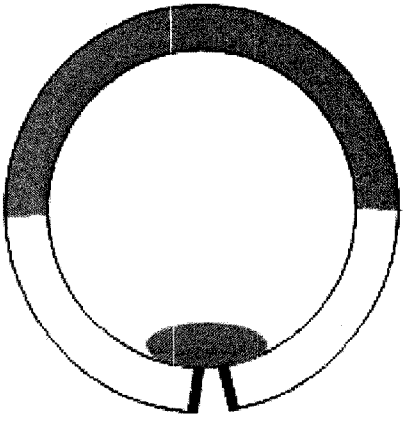

Germ band elongation

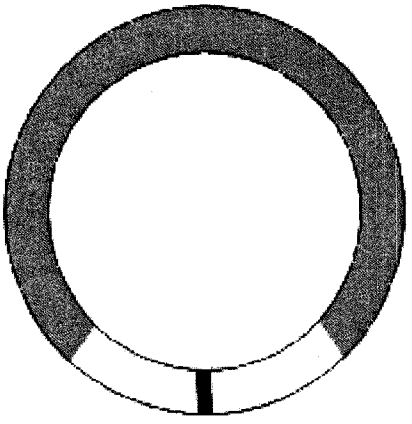

Neuroblast delamination

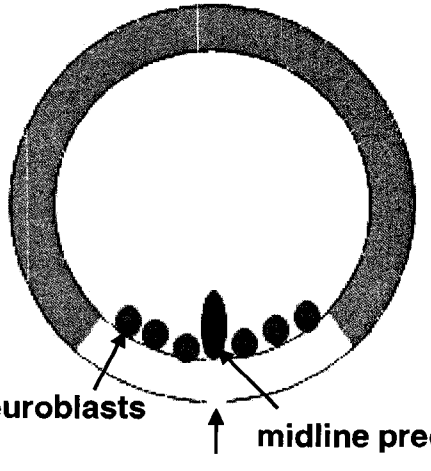

1.2.2 Gliogenesis

A number of different glial cell types can be found during CNS development. They are subdivided to two general classes: glia that prefigure and subsequently enwrap axon tracts and glia that adjoin and surround neuronal cell bodies (Goodman and Doe, 1993)

a) **Midline glial cells:** Three pairs of midline glia (MG) cells were identified from their presence before axon outgrowth in patterns which prefigure the first axon pathways. In each segment, the three pairs: MGA, MGM and MGP, surround the anterior and posterior commissures. The pioneer growth cones for the anterior and posterior commissures extend toward and make close contact with the end feet of the MG glial cells. After reaching their final positions, the glial cells enwrap the axon tracts in much the same way as vertebrate oligodendrocytes (Jacobs and Goodman, 1989). All ventral midline cells initially express *sim*, however, as glial cells begin to differentiate, detectable expression of *sim* becomes unique to the glial cells (Nambu *et al.*, 1990). The final position of these MG cells is exactly opposite to their positions at the time they are born, due to cell-specific migrations. These glial cells are important in establishing the normal patterning and shaping of axon commissures.

b) **Longitudinal glial cells:** The precursor glioblasts are identified from their expression of the *fushi tarazu* (*ftz*) gene in the neurogenic regions. Unlike neuroblasts which divide asymmetrically, the glioblasts divide to produce a pair of identical cells but also require regulation by the neurogenic genes surrounding it. The pair of glioblast progeny migrate medially, anteriorly and inwardly, they divide to six cells per segment that overlie the longitudinal axon tracts (Jacobs *et al.*, 1989). The cells

develop in two rows: one inner or medial (LGM) and the other outer or lateral (LGL). Pioneer growth cones of the longitudinal connectives extend along the elongate surface of the LG glial cells. In addition to *ftz*, the *prospero* (*pros*) gene is also expressed in the glioblasts, however unlike *ftz, pros* is present in the longitudinal glial progeny throughout embryongenesis (Doe *et al.*, 1991). Mutations in *pros* result in a disorganized array of longitudinal glial cells and the lack of longitudinal connectives, providing evidence that LG cells play a role in establishing the subsequent connectives (Goodman and Doe, 1993).

c) **Other glial cells:** Glial cells are also associated with both intersegmental and segmental nerve roots, four exit glial cells located just outside of the CNS and four peripheral glial cells have been identified. Several other lines of glial cells with unknown function have also been recognized, amongst which, some are not associated with axons but rather intermingled with neuronal cell bodies (Goodman and Doe, 1993).

1.2.3 CNS axon pathways

The development of axons in the nervous system requires axons to grow over complex pathways and long distances (Huber *et al.*, 2003;Dickson and Gilestro, 2006). To help find their way in the developing embryo, axon outgrowth begins with the extension of a highly motile and exquisitely sensitive amoeboid-like structure, the growth cone. These growth cones lead by detecting and responding to environmental cues that help guide them to their accurate targets. A wide variety of cell surface, extracellular matrix and secreted molecules can be used as guidance cues, in both an attractive and

Figure 2. The pattern of glia cells along *Drosophila* CNS. The *Drosophila* embryonic nervous system has a ladder-like structure consisting of longitudinal connectives (LC) and a pair of anterior and posterior commissures (AC and PC) per segment. Three pairs of midline glial cells (MGA, MGM, and MGP) surround the commissures. The longitudinal glial cells develop in two rows: one medial (LGM) and the other lateral (LGL). (Adapted from Goodman and Doe, 1993)

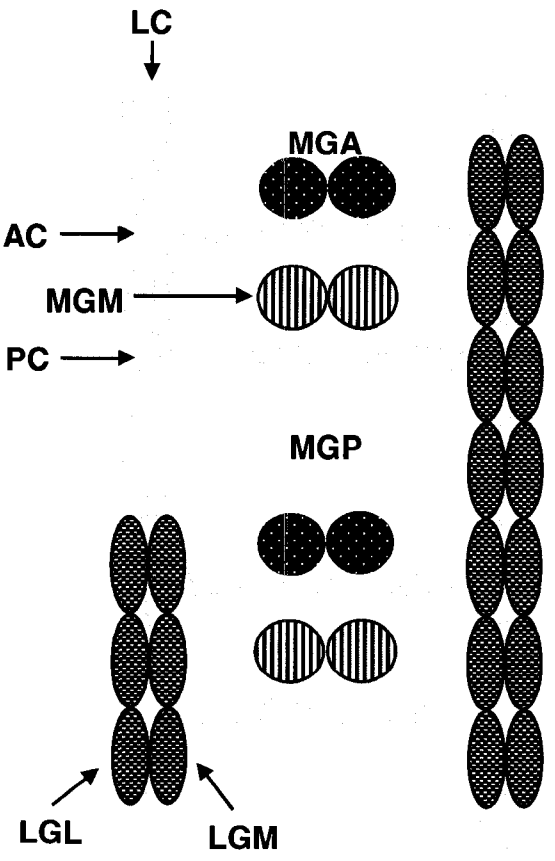
LC
MGA
AC
MGM
PC
MGP
LGL
LGM

repulsive manner, at close range or over long distances (Goodman and Doe, 1993;Dickson, 2002;Huber *et al.*, 2003).

Some CNS neurons project their axons ipsilaterally (on their own sides) as they pioneer or follow the first longitudinal pathways, however, most project contralaterally (across the midline via the commissural axons before turning either anteriorly or posteriorly) when projecting along a certain longitudinal pathway. Not surprisingly, the bulk of CNS neurons are commissural interneurons because they are required for formation of both axon tracts (Goodman and Doe, 1993).

a) **Commissural Pathways:** The construction of each neuromere begins when the first growth cones pioneer the CNS axon towards the midline forming commissures that connect the two symmetric halves of the nervous system (Goodman and Doe, 1993;Dickson and Gilestro, 2006). This process involves multiple signals emanating from the midline cells, both neurons and glia, to organize the guiding of the growth cones either toward the midline or prevent them from crossing the midline (Hummel *et al.*, 1999).

   The key attractive signaling of commissural axons to the midline is governed by the product of the *netrin* gene. Netrin, an evolutionary conserved chemo-attractant that binds to the receptor Frazzled (Fra), is secreted from the midline and initiates the passage of commissural axons to the midline. Both attractive and repulsive cues are essential for the correct establishment of commissures permitting the axons that have reached the midline boundary to leave and connect the two bilateral modules (Hummel *et al.*, 1999;Hiramoto and Hiromi, 2006).

Part of the repulsive function is mediated by upregulating the expression of Roundabout (Robo), a receptor for the midline repellent Slit (Sli). Robo proteins consists of an extracellular domain made of five immunoglobulin-like domains, the first two mapped as the Slit-binding site (Dickson and Gilestro, 2006). Slit is a large extracellular matrix protein produced almost exclusively by midline cells. It contains both leucine-rich repeat (LRR) and epidermal growth factor (EGF)-like repeats, which are known to play an important role in many aspects of eukaryotic cell control, including their involvement in extracellular events and ligand-receptor interactions (Rothberg *et al.*, 1990;Kidd *et al.*, 1999).

Mutations in *sli* result in improper differentiation of midline cells causing commissures and longitudinal axons to remain at midline; a similar phenotype is seen in *robo* mutants where too many axons cross the midline (Rothberg *et al.*, 1990;Brose *et al.*, 1999;Dickson and Gilestro, 2006). There is no strong evidence that commissural axons are more attracted to the midline than ipsilateral axons, however, ipsilateral axons are repelled by Sli, acting as a short-range repellent signaling through Robo and preventing ipsilateral axons from crossing the midline. Robo is highly detected on the growth cones of ipsilateral pioneers but barely detectable on commissural pioneers as they extend across the midline despite the presence of *robo* mRNA in both axons. However, once commissures reach the contralateral side, high levels of Robo protein are identified. (Brose *et al.*, 1999;Dickson, 2002).

A third gene, *commissureless* (*comm*), regulates Robo protein levels during midline crossing in *Drosophila*. *Comm* mutants have the opposite phenotype to *robo*, where no axons cross the midline at all, commissures are present but form

Figure 3. Roles of Netrin and Slit–Robo signalling in the crossing of commissural axons. Top panel: Netrins at the midline attract axons by binding to the Fra receptor, whereas Robo is silenced by sorting processors such as Comm to prevent the repulsion of commissural axons from the midline. **Middle panel:** at the midline, Robo, in response to Slit, silences Netrin, thereby preventing axons from stalling at the midline, expelling the axon from the midline. **Bottom panel:** once axons have crossed the midline, high Robo levels on the axons prevent them from re-crossing the midline at the same time Robo represses Fra so there is no longer an attraction to the midline. (Adapted from Carmeliet and Tessier-Lavigne, 2005)

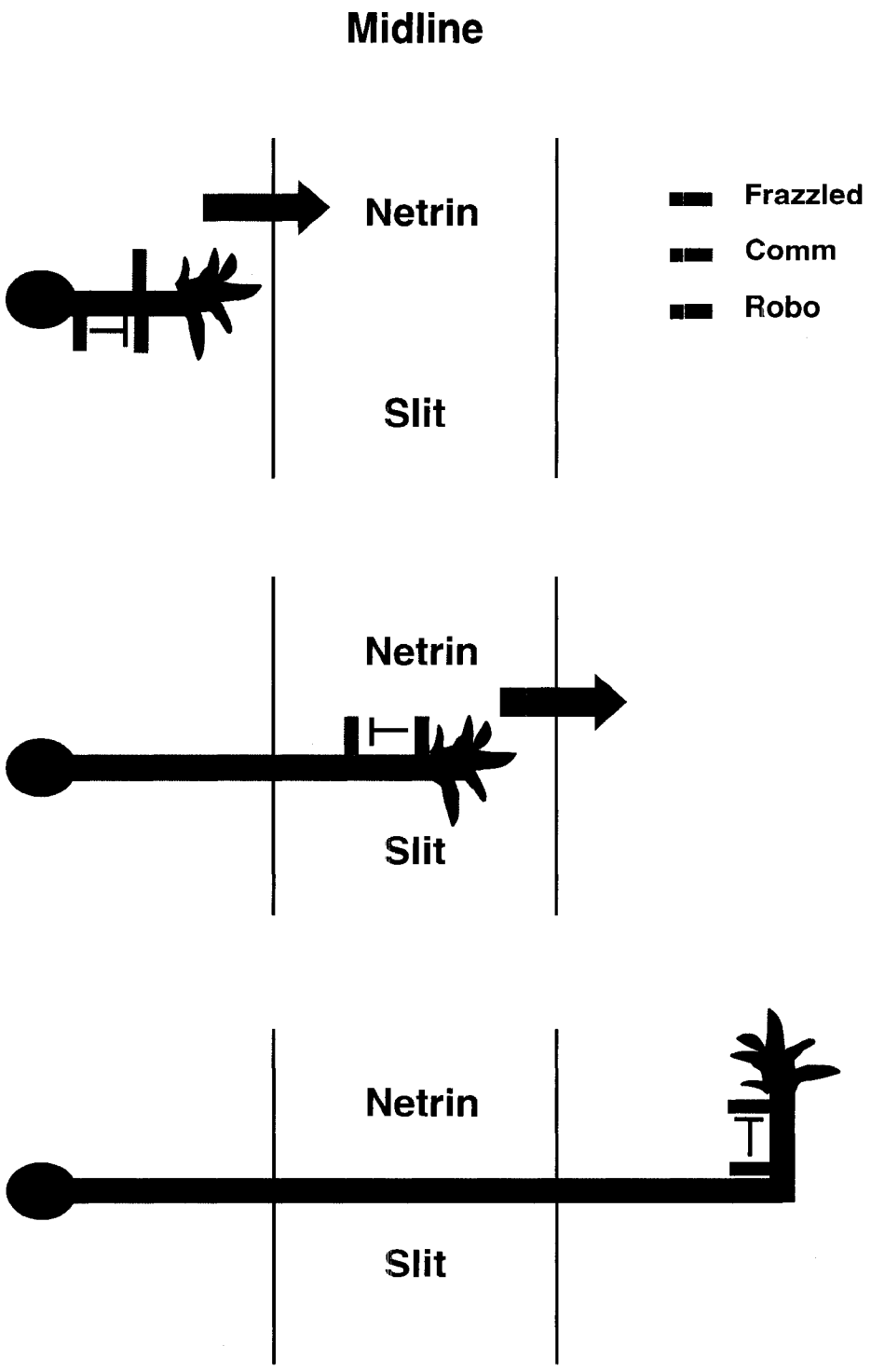
Midline
Netrin
Slit
Frazzled
Comm
Robo
Netrin
Slit
Netrin
Slit

ipsilaterally instead (Tear *et al.*, 1996;Dickson and Gilestro, 2006). Comm is known as a sorting processor for Robo as it controls normal commissural crossings by down-regulating the levels of Robo protein in the growth cones. Once they have crossed, down-regulation of Comm allows Robo upregulation, this represses the chemo-attractant binding site, Fra, thus ensuring that commissural axons do not re-cross the midline again (Brose *et al.*, 1999;Keleman *et al.*, 2002).

b) **Longitudinal Pathways:** During development of longitudinal connectives a small number of early ipsilateral interneurons, mostly MP1, dMP2, vMP2 and pCC, pioneer a scaffold of longitudinal fascicles that are subsequently joined by other ipsi- and contralateral axons projecting in anterior or posterior directions (Sanchez-Soriano *et al.*, 2007). The growth cones of these early interneurons establish an intimate contact with longitudinal glia cells found in the area of the future connectives prior to the axonal growth phase.

Although precise guidance molecules specific to longitudinal axon navigation in *Drosophila* are not known, evidence suggests that the mechanisms of longitudinal navigation are linked to those involved in bilateral connection, including Netrin and Robo proteins. For example, as Netrin is guided to the midline by Fra, dMP2 longitudinal neurons turn posteriorly to avoid the Netrin-positive region but instead track along its edge (Goodman and Doe, 1993;Hiramoto and Hiromi, 2006).

In addition, longitudinal projecting axons are positioned at certain locations within the connectives, revealing the ability of axons to mediate selective fasciculation (ability to distinguish one bundle of fascicles from another) (Goodman

and Doe, 1993;Sanchez-Soriano *et al.*, 2007). Like the commissural axons, both short-range interactions and long range organiser activity contributes to the arrangement and maturity of longitudinal fascicles.

1.3 Development of the tracheal system

Branching tubular epithelial structures are important to most animals for the transport of gases and liquids throughout the body (Samakovlis *et al.*, 1996). Many of the major organs, such as lung, kidney and vascular system, are designed in a branched network. These networks contain thousands or millions of branches, rendering it difficult with the limited prospects for genetic analysis to study the developmental mechanisms and molecules that control the branching processes in mammals. On the other hand, the tracheal system of *Drosophila* makes an excellent model system given that it is fairly simple in structure and provides accessible genetics to assist the progress in understanding branching morphogenesis (Jazwinska *et al.*, 2003).

The tracheal branches in *Drosophila* embryos are made of an epithelial monolayer surrounding a central lumen through which gases flow. Oxygen enters through the anterior and posterior spiracular openings, passes through primary, secondary and terminal branches to reach the tissues (Jarecki *et al.*, 1999). The tracheal network also displays bilateral symmetry following a repeated segmental organisation (Ghabrial *et al.*, 2003). Development of the network stems from 10 clusters of roughly 80 tracheal precursor cells distributed in every thoracic and abdominal hemisegment of the embryo (Tr1-Tr10). The clusters are known as tracheal placodes or pits and undergo similar

developmental events to give rise to a hemisegment of the tracheal system (Samakovlis *et al.*, 1996).

Six primary tracheal branches bud out in different directions and to characteristic lengths from each placode sac derived from invaginated ectoderm (Samakovlis *et al.*, 1996). The direction corresponds to six distinct primary branches: dorsal branch, dorsal trunk anterior and posterior, visceral branch, lateral branch anterior and posterior (Jazwinska *et al.*, 2003). This is followed by the sprouting of two-dozen secondary branches. The pattern of primary and secondary branch budding is highly stereotyped and controlled (Ghabrial *et al.*, 2003). As secondary branches begin to sprout hundreds of fine terminal branches (tracheoles), the developmental scheme becomes more variable and regulated based on tissue oxygen demand in the body (Samakovlis *et al.*, 1996).

Cells left in the placodes which do not grow to form primary branches remain to form the transverse connectives; similarly, not all primary and secondary branches complete the branching sequence, specific branches cease branching and grow to interconnect the tracheal network (Samakovlis *et al.*, 1996;Ghabrial *et al.*, 2003). The dorsal trunk is formed by the fusion of the dorsal trunk anterior and posterior primary branches.

1.3.1 Transcription Factors Trachealess::Tango

Before branching can begin, tracheal precursor cells must be selected in the embryonic ectoderm. *trachealess* (*trh*) selects the tracheal primordial just before the first morphological signs of their specialization; it is the earliest tracheal-specific marker known (Metzger and Krasnow, 1999;Ghabrial *et al.*, 2003). *trh* encodes a bHLH–PAS protein family and is expressed in all tracheal cells throughout development (Sonnenfeld

et al., 1997). The initiation of tracheal development is complete when this heterodimeric transcription factor forms a complex with the bHLH-PAS complex of Tgo. Following the same principles as the Sim::Tgo complex to initiate CNS transcription, the Trh::Tgo complex binds to CME present in the promoter region of its target tracheal gene to initiate expression (Sonnenfeld *et al.*, 1997;Ohshiro and Saigo, 1997)

The Trh::Tgo heterodimer now regulates the expression of proteins responsible for sac formation, as well, prepares the sacs for the branching events that follow by triggering the required genes (Metzger and Krasnow, 1999;Ghabrial *et al.*, 2003). *trh* mutants show that many of the early tracheal genes are not induced, including the indispensable *breathless (btl)* target, a *Drosophila* homolog of mammalian fibroblast growth factor (FGF) receptor found throughout the sacs (Metzger and Krasnow, 1999;Ghabrial *et al.*, 2003). A previous experiment by Ohshiro and Saigo demonstrated with both biochemical and genetic evidence that Btl directly interacts with Trh::Tgo heterodimers via its three CME in the minimum enhancer region (Ohshiro and Saigo, 1997).

1.3.2 Branchless/Breathless

btl is required at the initiation of tracheal cell migration and is expressed in tracheal precursors during invagination and branching for primary, secondary and/or terminal branch formation (Chiang *et al.*, 1995;Metzger and Krasnow, 1999;Ohshiro *et al.*, 2002). However, the most notable gene involved in branching morphogenesis is the *branchless (bnl)* gene, a critical determinant of the branching pattern. It encodes a *Drosophila* FGF that serves as ligand for Btl and is homologous to mammalian FGF-10; its developmentally regulated distribution is responsible for the spatially restricted

Figure 4. Trh::Tgo heterodimer regulates trachea formation. Trh and Tgo are bHLH-PAS proteins that form a heterodimer complex. The complex enters the nucleus and binds to CNS midline enhancer elements (CME) present in the promoter regions of their targets. The target gene shown here is the FGFR known as *breathless* (*btl*). (Adapted from Crews, 1998)

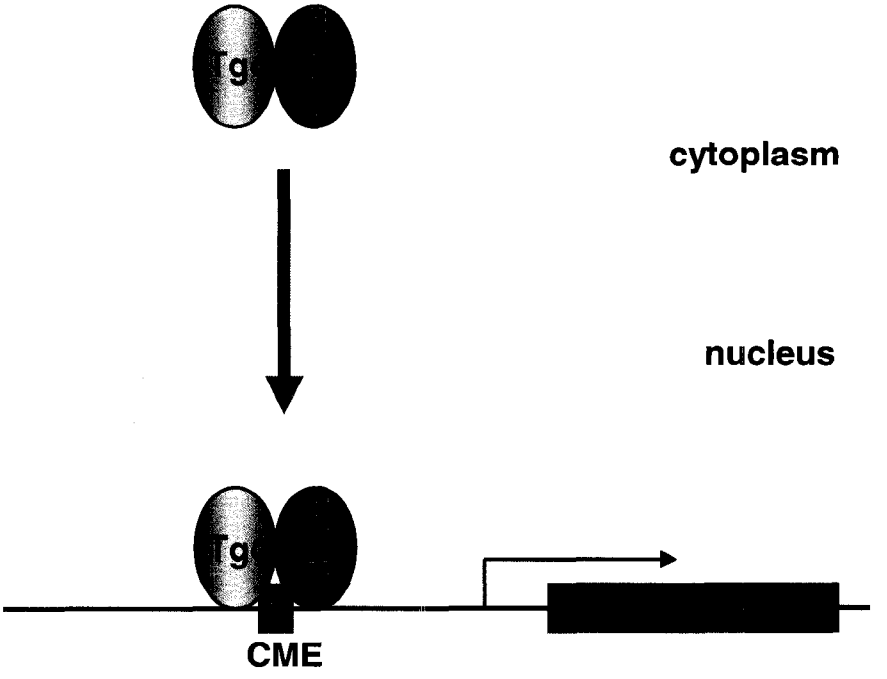
Tg
cytoplasm
nucleus
Tg
CME

activation of Breathless (Metzger and Krasnow, 1999;Ohshiro *et al.*, 2002;Ghabrial *et al.*, 2003).

1.3.3 Primary branching

Prior to primary branching, *btl* is turned on in tracheal cells by Trh/Tgo. The ligand *bnl* is also expressed at the same time but not in the same locations, rather in small clusters of epidermal and mesodermal cells arranged around each tracheal sac. The expression of Bnl is considered to serve as a motogen or chemoattractant for tracheal cell migration, since their positions dictate where the primary branch will bud (Ohshiro and Saigo, 1997).

As the strong *bnl* FGF centres are turned on, tracheal cells begin to migrate towards them, and when *bnl* expression is turned off, the branching in turn stops (Ghabrial *et al.*, 2003). If *bnl* is expressed in more distal clusters, the branch will continue to migrate towards the new patch (Metzger and Krasnow, 1999). In experiments where *bnl* is mis-expressed in novel positions, ectopic branch growth will occur pursuing all the pathways designated by *bnl* (Reichman-Fried and Shilo, 1995); consequently, in *bnl* or *btl* mutants, no sign of primary branching is observed. These results demonstrate that primary branch budding and outgrowth is positioned by the pattern of *bnl* expression as Branchless FGF is a dynamic chemoattractant for tracheal cells.

Once the secreted Bnl FGF ligand binds to a Btl receptor on nearby tracheal cells, the receptor's tyrosine kinase activity is stimulated and activates the Ras/MAPK cascade (Ghabrial *et al.*, 2003). The *btl* gene creates a positive feedback loop to maintain the expression of the receptor in areas of active signaling, which in turn, induces the

expression of secondary branching genes needed for the next step in tracheal development (Ghabrial *et al.*, 2003).

1.3.4 Secondary branching

Similar to primary branching, secondary branching is also controlled by *bnl* and *btl*, but involving a different molecular mechanism. As primary branches extend toward the Branchless FGF signaling centres, cells at the growing end are exposed to high levels of the signal, triggering expression of secondary branch genes at the tips. One such gene is an ETS domain transcription factor called *pointed*, a required gene for secondary branching (Sutherland *et al.*, 1996;Ghabrial *et al.*, 2003).

To prevent all cells receiving Branchless FGF signal from forming secondary branches, FGF signaling also activates genes that inhibit branching, as seen in the case of *sprouty* (*spry*). Expression of *spry* blocks Branchless signaling to more distant tracheal cells, thereby limiting secondary branch sprouting to positions closest to the FGF signaling sources (Metzger and Krasnow, 1999).

1.3.5 Terminal branching

Several hours after secondary branches are formed; the extremely fine terminal branches begin to expand and continue throughout the larval life. Unlike primary and secondary branching, terminal branching pattern is vastly variable and mainly determined by oxygen physiology rather than fixed developmental control, comparable to angiogenesis in mammals (Ghabrial *et al.*, 2003). It has been determined that low oxygen stimulates formation of terminal branches and high oxygen inhibits it (Metzger and Krasnow, 1999). This phenomenon is actually controlled by Bnl FGF as well.

Even though *bnl* expression is turned off once secondary branches begin to grow and the first terminal genes begin to be expressed, it turns on a few hours later at the beginning of larval life (Ghabrial *et al.*, 2003). The most dramatic change in branch patterning found at this stage results from the switch from developmental to physiological controls of *branchless* expression (Jarecki *et al.*, 1999). *bnl* expression is stimulated by low oxygen levels; the secreted FGF behaves as a branch inducer to guide new terminal branches to signaling oxygen-starved cells to relieve hypoxia. In addition, to *bnl* the final pattern of terminal branching requires new genes to change the expression pattern of the FGF ligand, rendering it oxygen-sensitive (Metzger and Krasnow, 1999) . One such gene is *blistered*, also known as *pruned*, a *Drosophila* homologue of mammalian serum response factor (SRF), coding for a MADS domain containing protein proposed to function with a ternary complex factor as part of an FGF-activated transcription complex (Guillemin *et al.*, 1996;Metzger and Krasnow, 1999).

The *blistered* gene which is turned on just before terminal branching begins is triggered by Bnl FGF signaling from the previous round of branching. The dSRF like its mammalian homologue in molecular structure, forms a similar transcription complex in terminal cells, which in turn regulates and induces expression other genes required for terminal branch formation (Guillemin *et al.*, 1996;Metzger and Krasnow, 1999;Jarecki *et al.*, 1999;Ghabrial *et al.*, 2003).

1.4 *Drosophila* eye

Like other arthropods, adult *Drosophila* possess highly structured compound eyes built from about 800 individual ommatidia units each displaying precise polarity (Strutt

and Mlodzik, 1995;Lloyd *et al.*, 1998). Each ommatidium can be described as a small camera focusing on a different point in space to produce a mosaic image of the world. The "film" consists of eight photoreceptor neurons, arranged in a ring with six outer cells to capture light and transmitting neural impulses to the brain (Strutt and Mlodzik, 1995;Moses, 2003).

An outcome of this complex structure is that the *Drosophila* eye is very sensitive to imperfections. The slightest change in shape, location and/or numbering of the cells will disrupt the ability to capture an image. Thus, the development of these eyes is exquisitely precise, and any gene mutation that affects any of these cell characteristics, even slightly can result in a rough eye phenotype (Moses, 2003). The presence of >6000 neurons, the potential for easily observable phenotypes and the power of *Drosophila* genetics makes the *Drosophila* eye an extremely useful tool with which to study many aspects of neural development (Frankfort and Mardon, 2002). Blindness triggered by genetic screens with such eye mutations does not necessarily harm any other aspects of the fly's health, moreover, virtually all of the genes required for proper *Drosophila* eye development are highly conserved, and many perform similar functions in a wide range of species (Frankfort and Mardon, 2002).

1.5 *jing*

One gene found repeatedly in several different *Drosophila* developmental processes is *jing*. Presently, *jing* is recognized as an essential protein for controlling the differentiation and survival of cells in the CNS midline, the trachea and brain during embryogenesis (Sedaghat and Sonnenfeld, 2002;Sonnenfeld *et al.*, 2004). The Jing

protein is characterized as a zinc-finger transcription factor with C_2H_2 zing fingers most similar to the mouse protein AEBP2, a CCAAT enhancer binding protein (C/EBP) (Sedaghat *et al.*, 2002). *jing* was first identified to function in the *slow border cell* (*slbo*) pathway from a screen testing for mutations that cause border cell migration defects in mosaic clones. It was found to be a nuclear factor that when mutated resembles the phenotypes of *slbo* mutants but is distinct from other classes of border cell migration mutants (Liu and Montell, 2001). Both mutants disrupt the *Drosophila* C/EBP gene expression.

One important form of cellular regulation occurs at the transcriptional activation level. It has been established that Jing accumulates in the embryo after stage 9 and localizes to the nuclei of CNS midline and trachea cells (Sedaghat *et al.*, 2002). Combined with its potential DNA-binding and transactivation domains, Jing may perform a transcriptional regulatory role required for the differentiation and survival of these CNS midline and tracheal precursors (Sedaghat *et al.*, 2002). A genetic approach by employing *jing* loss-of-function confirmed *jing*'s role in the commitment of CNS midline and tracheal cells. *jing* mutants were found to genetically interact with *tgo* and *sim* mutants and their target *sli* in the CNS. In the trachea, *jing* mutants were found to genetically interact with *trh* mutants and its target *btl* (Sedaghat *et al.*, 2002).

1.5.1 Role of *jing* in the CNS midline

Analysis of homozygous *jing* mutant embryos reveals that CNS midline neurons and glia do not differentiate properly. Embryos double mutant for *jing* and *sim* display a CNS phenotype similar to that of *sim* homozygotes, implying that *jing* functions downstream of *sim* (Sedaghat *et al.*, 2002). The importance of *sim* to induce all midline

gene expression has already been established (Nambu *et al.*, 1990). Homozygous *jing* mutants display reductions in CNS midline cells, leading to a loss of longitudinal connectives and improper separation of commissures (Sedaghat *et al.*, 2002). Further investigations reveal that there are more apoptotic glia in Jing homozygotes during stage 12 than in wild-type embryos, resulting in the loss of midline gene expression in *jing* mutants (Sedaghat *et al.*, 2002).

Since the differentiation of CNS midline cells is regulated by the epidermal growth factor receptor (EGFR) (Nambu *et al.*, 1990), studies were conducted in search of a functional relationship between *jing* and the EGFR. Several observations revealed that *jing* is intimately involved in EGFR signalling in the midline glia. First *jing* mutant embryos fail to maintain MAPK activity and *Egfr* expression in midline cells (Sonnenfeld *et al.*, 2004). Second, *jing* can induce *Egfr* transcription in the midline, producing a similar over-expression phenotype in glial survival as other over-expressed EGFR pathway genes (Sonnenfeld *et al.*, 2004). In addition, *jing* mutants can be partially rescued by gain-of-function *Egfr* or a transgenic copy of the activated EGFR pathway protein Ras1, decreasing the number of homozygous *jing* embryos with midline cell death (Sonnenfeld *et al.*, 2004). Together, these findings are consistent with the hypothesis that *jing* functions upstream in the *Egfr* pathway in CNS midline glia.

1.5.2 Role of *jing* in the trachea

The presence of Jing protein in many tracheal cells was interesting given the critical function of Trh::Tgo heterodimers in the same cells. This raised the possibility that *jing* may be a conserved component of bHLH-PAS-mediated transcriptional regulation. *jing* has multiple roles during tracheal morphogenesis. From the early stage

of allocating the correct number of cells to the tracheal plaocdes, to *jing*'s presence within the nuclei promoting the differentiation of precursors, loss of *jing* results in a defective patterning of tracheal lineages (Sedaghat *et al.*, 2002). However, the most severe effects of loss of *jing* appear in the dorsal trunk and visceral branch development.

Egfr expression has also been clearly identified in *Drosophila* tracheal cells. During stage 10, EGFR signalling is activated in the central region of the tracheal placode by transcription of *rhomboid* (*rho*), an EGF pathway activator required for complete tracheal placode invagination and a target of Trh/Tgo transcription factors (Ghabrial *et al.*, 2003). Rho is known to process the EGFR pathway ligand Spitz and is responsible for the formation of anteroposterior branches including the dorsal trunk and visceral branch (Wappner *et al.*, 1997;Sonnenfeld *et al.*, 2004). As seen in CNS midline development, there is a critical role for the *Egfr* pathway in the developing trachea. Mutations in the Rho and Spitz result in similar phenotypes showing a failure in development of tracheal branches; specifically, the dorsal trunk and visceral branch are missing or incomplete (Wappner *et al.*, 1997).

Given the importance of EGFR in the dorsal trunk and visceral branch, it is no surprise to find that defects in dorsal trunk and visceral branch formation in *jing* mutant embryos are similar to those in embryos homozygous mutant for *Egfr* signalling (Sedaghat *et al.*, 2002). The Jing mutant phenotype consists of breaks in the dorsal trunk and reduction in visceral branch formation (Sonnenfeld *et al.*, 2004). Conversely, since mutations in *Egfr* pathway genes do not affect tracheal placode cell numbers, it can be assumed that *jing* may function prior to EGFR signalling (Sedaghat *et al.*, 2002).

Further proof that *jing* and *Egfr* pathways are inter-dependent during trachea morphogenesis was found from gene dosage analysis. In embryos double heterozygous for *jing* and *Egfr* genes, defects should only arise when one copy of each gene interacts with the other. Breaks in dorsal trunk, consistent with the homozygous phenotypes of *jing* and *Egfr* pathway mutants, were observed in the double heterozygous embryos (Sonnenfeld *et al.*, 2004). Therefore, proper *Egfr* pathway and *jing* function are required to regulate signal transduction in developing midline and tracheal cells.

1.6 Interactors of *jing*

The role of *jing* in controlling cell survival and differentiation in both CNS midline and trachea through EGFR signal transduction has been demonstrated (Sedaghat *et al.*, 2002;Sonnenfeld *et al.*, 2004). However, the transcriptional mechanisms underlying Jing function are not known. Therefore, in order to gain a more comprehensive view of the functions and molecular mechanisms of *jing*, a genetic screen by the use of a gain-of-function (GOF) assay was carried out in the developing eye-imaginal disc. A total of 591 individual third chromosome EP lines were screened, seven of which were documented to specifically interact with *jing* during ommatidia formation (Sun *et al.*, 2006). Of the seven, EP(3)3354 produced one of the stronger interactions with *jing* (Figure 5) and was found to be inserted in the 5' regulatory region of a gene encoding a MADF regulatory domain, thus earning the name JIGR1 (***j****ing* **I**nteracting **G**ene **R**egulatory **1**).

1.6.1 Gain-of-function assay

The Berkeley *Drosophila* Genome Project (BDGP) began in hopes of sequencing the euchromatic genome of the four *Drosophila* chromosomes. Nevertheless, model organism genome projects are only useful if they are accompanied by genetic studies to determine functions of the sequenced genes, contributing to better assess human DNA sequences. The BDGP gene-disruption project started as a technique in answer to the problems of disrupting a particular gene or identifying the open reading frame (ORF) responsible for a mutant strain's interesting properties (Spradling *et al.*, 1995). The project involved a large collection of *Drosophila* strains each with a single, genetically engineered P transposable element inserted in a defined region. The inserted P elements in BDGP lines carry enhancer traps, or Upstream Activating Sequences (UAS) elements, that can be used to efficiently acquire information about the expression pattern of disrupted genes (Spradling *et al.*, 1995).

In conventional genetic screens, mutagens typically reduce or eliminate gene function, however, it has long been recognized that rare gain-of-function mutations can be extremely informative about gene function (Rorth *et al.*, 1998). While loss-of-function phenotypes could be lost due to functional redundancy, gain-of-function may provide more help.

Genes that are tagged with a UAS-containing P-element insertion can be mis-expressed when combined with a GAL4 regulatory element. The GAL4 will direct expression of any gene that happens to lie next to the P-element insertion site (Rorth *et al.*, 1998) (Figure 6). This provides a powerful tool to control targeted gene expression in both a temporal and spatial fashion in vivo (Duffy, 2002). Based on this premise,

Figure 5. Gain-of-function assay to identify *jing*-interactors in the *Drosophila* eye. Transgenes were driven by *gmr-Gal4*, compound eyes are shown in scanning electron micrographs. **(A)** Wildtype eye. **(B)** Over-expression of EP(3)3354 showed a mildly rough phenotype. **(C)** Over-expression of *jing*. **(D)** A more severe rough eye phenotype was present when EP(3)3354/*jing* were co-expressed indicating a genetic interaction.

A
B
100 µ
C
D

Figure 6. Gal4/UAS bipartite system. The UAS/GAL4 ectopic expression system allows for cell- and tissue-specific over-expression of transgenes in *Drosophila melanogaster*. This bipartite expression system contains the yeast transcription factor, GAL4, and its target sequence, UAS, to which GAL4 binds in order to activate gene transcription. Expression can be in many different patterns by control of various promoter sequences. (Adapted from Brand and Perrimon, 1993)

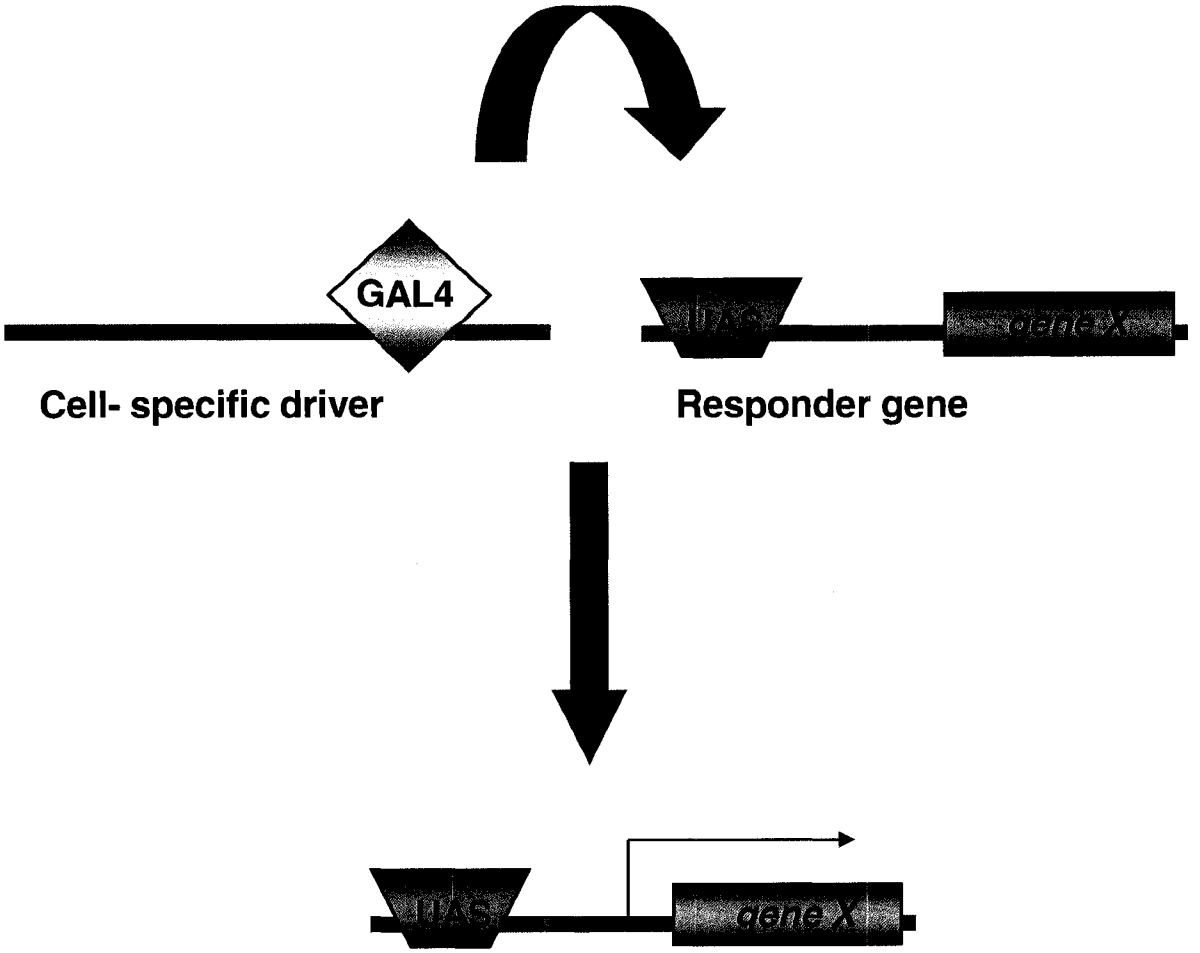

Transcriptional activation of *Gene X*

additional factors important to *jing* function were explored with a set of enhancer/promoter-tagged (EP) genes found on the third chromosome (Sun *et al.*, 2006).

A study has already commenced in another of the seven *jing*-interactors. The *Drosophila* homologue of the human α-thalassemia and mental retardation X-linked gene *DATR-X* was explored in CNS formation and was observed to be functionally related to *jing*, as well, required in axon guidance and glial survival. This indicates *jing* interactors not only offer more depth to *jing* functions and mechanism, they may also, in their own right, be influential players in *Drosophila* CNS development with relevance to vertebrate genes.

1.7 *JIGR1*

EP(3)3354 or *JIGR1* was chosen for a more thorough characterization of its properties and functions. The better the genes which interact with *jing* are understood, the better the full influence of *jing* in *Drosophila* can be recognized. The EP element in *JIGR1* lies upstream of the transcript identified as CG17383, coding for a relatively short protein consisting of 336 amino acids (aa) in length. A quick database query through the web tool SMART (Simple Modular Architecture Research Tool: http://smart.embl.de/) identifies that within the 336 aa, JIGR1 contains strictly one conserved domain which has a homology to the MADF protein domain.

1.8 MADF domain

MADF stands for Myb/SANT-like domain in Adf-1 and was first documented in Adf-1, a transcriptional activator of alcohol dehydrogenase. Soon after, the importance

of Adf-1 in *Drosophila* biology increased when it was found to bind to the promoters of a diverse group of developmentally regulated genes (England *et al.*, 1992;Ljunggren *et al.*, 2006;Zimmermann *et al.*, 2006). Although the list of MADF containing proteins has expanded since then, very few of them have been experimentally characterized.

In addition to Adf-1, another transcriptional regulator of *Drosophila*, Dorsal-interacting protein 3 (Dip3), also contains a MADF domain. Dip3 functions as a co-activator to stimulate synergistic activation of the dorsoventral axis formation regulators, Dorsal and Twist (Bhaskar and Courey, 2002). Both Adf-1 and Dip3 possess MADF domains that can bind to DNA directly as shown by experiments conducted by the Cutler team and Bhaskar team respectively (Cutler *et al.*, 1998;Bhaskar and Courey, 2002). MADF has been repeatedly categorized as a subfamily of the Myb/SANT domain (England *et al.*, 1992;Bhaskar and Courey, 2002). The overall amino acid homology between MADF and SANT domains is weak, with a stronger homology between the MADF domain and the portion of the second c-myb SANT domain. This homology is significant because it includes two highly conserved tryptophans (boxes) and a cluster of basic residues that may play important roles in DNA recognition and binding (England *et al.*, 1992;Bhaskar and Courey, 2002).

1.9 Rationale of this project

Undeniably, the *jing* zinc-finger transcription factor plays an essential role in CNS midline and tracheal cell differentiation through controlling growth factor signaling in *Drosophila* (Bhaskar and Courey, 2002;Sedaghat *et al.*, 2002;Sonnenfeld *et al.*, 2004). Loss of *jing* leads to defective neuronal and glial differentiation resulting the death of

embryonic CNS midline (Sedaghat and Sonnenfeld, 2002). Equally important is the role of *jing* in tracheal tubule patterning, without which, defects and inappropriate apoptosis are found during tracheal cell development (Sedaghat *et al.*, 2002). However, since the mechanisms of action for *jing* are not fully characterized, it is imperative to acquire a full working model to provide explanations for all the phenotypes associated with *jing* mutant embryos. The *Drosophila* model system is capable of producing a plethora of novel and/or refined insights into relevant molecular mechanisms that are also conserved in higher organisms (Sanchez-Soriano *et al.*, 2007). Given that a *jing* homolog has been found in vertebrates, a complete understanding of this gene should contribute valuable and beneficial data to developmental biology on the whole, giving insight to the more complex vertebrate pathway formation processes.

1.10 Statement of hypothesis and objectives

The hypothesis for this study was: the *jing* interactor *JIGR1* functions with *jing* in the development of trachea and CNS during embryogenesis. I tested this hypothesis with the following objectives:

Objective 1. Examine genetic interactions between *JIGR1* and other *jing*-interacting genes in *Drosophila* adults.

Objective 2. Analyze embryonic *JIGR1* expression via *in situ* hybridization.

Objective 3. Produce a polyclonal antibody specifically recognizing *JIGR1*

Objective 4. Determine the role of MADF in localization of JIGR1 within the cell.

Objective 5. Investigate the MADF domain in *JIGR1* and its homologues.

Objective 6. Analyse JIGR1 gain-of-function phenotypes in both CNS and tracheal development.

Objective 7. Assess the relationship of *JIGR1* and *jing* under *in vitro* conditions.

MATERIALS AND METHODS

2.1 *Drosophila* strains

The collection of third chromosome transgenic EP strains, including EP(3)3354, was obtained from the Hungarian Szeged stock centre. This collection was generated and acquired from Rorth (Rorth, 1996). *gmr-Gal4* (second chromosome) was obtained from J. Nambu (Hay *et al.*, 1994). The following stocks were obtained form the Bloomington *Drosophila* Stock Center at Indiana University: w^{118}, glial driver *gcm-Gal4* (Freeman *et al.*, 2003), *JIGR1*deficient flies *Def(3R)Exel6203* with absent cytogenetic region 96E2-96E6, and *paired-Gal4* (Dierick and Bejsovec, 1998). *jing* lethal mutant, $jing^3$ flies, were provided by M. Sonnenfeld (Sedaghat *et al.*, 2002). Flies were raised on standard cornmeal medium at room temperature, 25 °C.

2.2 Identification and classification of *JIGR1*

A genetic interaction between EP(3)3354 and *jing* was first identified in a gain-of-function assay in the adult eye as described by X. Sun (Sun *et al.*, 2006). On the BDGP database, the cDNA for CG17383 was documented as the associated gene found downstream of the P element in the EP(3)3354 insertion strain. The cDNA was documented as encoding a transcription factor containing a MADF domain. A search of additional homologues was performed using the BLAST program (http://www.ncbi.nlm.nih.gov). Both full-length translated JIGR1 and JIGR1 conserved domain, MADF, were aligned with *Drosophila pseudoobscura* protein GA14496-PA and its MADF domain respectively using CLUSTAL X. Predicted protein domains of JIGR1 were analyzed using SMART Sequence Analysis (http://smart.embl-heidelberg.de).

2.3 Interaction assays

Males from EP(3)635, EP(3)3084, EP(3)3145 and EP(3)3354 were crossed with female *gmr-Gal4* virgins. For the analysis independent of EP line interaction effects, 1 to 3 day old adult heads from the F_1 progeny were collected for dissection, fixation (4% formaldehyde, 2% gluteraldehyde) overnight at 4 °C, followed by three 15min washes and finally dehydration (ethanol series). Following the same procedures, interaction assays were conducted when the F_1 progeny of EP(3)3354 was crossed in turn with each of the other EP F_1 progeny. All the dehydrated samples were sent to the Mount Sinai Bioimaging Centre (Toronto) for sputter coating with gold-palladium for SEM examination and toluidine blue stained for cross-sectioning and light microscopic analysis.

2.4 Antibodies and immunostaining of *Drosophila* embryos

Embryo fixation and staining were performed according to standard protocols (Patel, 1994). Embryos from various stages in development were collected daily at room temperature (RT). Embryos were dechorionated by 50% bleach, fixed in a solution containing 4% formaldehyde for 30min and stored in MEOH at -20 °C until staining. When the collection of embryos was sufficient, they were washed thoroughly with PBT (1X PBS; 0.1% Triton X-100) to replace all traces of MEOH. An overnight incubation with the primary antibody at 4 °C followed a half hour block with 5% normal goat serum. For diaminobenzidine histochemistry, a horseradish peroxidase-conjugated (goat anti-mouse IgG or goat anti-rabbit IgG) secondary antibody was added at a 1:100 dilution for 2h (Kim *et al.*, 1998), 300 µl of diaminobenzidine/PBT (DAB, Sigma) at a 1:3 ratio was

added before oxidization with 3µl of H_2O_2. For fluorescence microscopy, a FITC-conjugated secondary antibody (Jackson ImmunoResearch) was supplemented at a 1:100 dilution. The stained embryos were dehydrated with a series of ethanol washes and mounted in methyl salicylate and Vectashield medium (Vector Laboratories) respectively. Images were examined by Nomarski optics on a Zeiss Axioskop microscope and captured on a Nikon DXM1200 digital camera.

The following antibodies were obtained from the Developmental Studies Hybridoma Bank (Iowa City, IA): BP102 (1:5) and 2A12 (tracheal tubules 1:3).

2.5 *In situ* hybridization

A digoxigenin-labelled RNA probe was generated for whole-mount *in situ* hybridizations. Full length JIGR1 cDNA (LD33329 from BDGP) with hemagglutinin (HA) protein tag fused at the C-terminus was subcloned into pCR 2.1-TA vector (Invitrogen) in both directions with *KpnI* and *XbalI* restriction enzymes. Antisense probe was synthesized using the T7 promoter when JIGR1 was cloned in a 3' to 5' direction; the same method was repeated with vectors containing JIGR1 cloned in a 5' to 3' direction to generate the sense probe. T7 RNA polymerase was provided by Genius 4 RNA Labelling Kit (Roche) and used according to manufacturer's directions. Probe specificity was determined in embryos over-expressing EP(3)3354 through the action of *prd-Gal4* drivers.

Embryos at all stages were prepared for hybridization by dechorionating in 25% bleach, fixed in 4% formaldehyde and stored in MEOH. *In situ* hybridization was carried out following the protocol described by X. Sun (Sun *et al.*, 2006). In brief, embryos were

washed in PBT (PBS; 0.05% DEPC; 0.1% Tween 20) to replace the MEOH and post-fixed with 4% formaldehyde. Digestion with 0.05% Proteinase K was applied for 5min and stopped in 2mg/ml glycine. Hybridization B solution (50 % formamide; 25% 20X SSC; 25% DEPC in H_2O) substituted PBT before embryos were prehybridized with hybridization A solution (50% formamide; 25% 20X SSC; 10 mg/ml sonicated salmon sperm DNA; 20 mg/ml tRNA; 100 mg/ml heparin) for 1h. 2 µl of probe was added and incubated at 70 °C overnight. The next day, a pre-absorbed anti-DIG antibody conjugate was applied to the embryos for 2h to label the probe. Lastly, embryos were washed in a pre-staining buffer (1M $MgCl_2$; 5M NaCl; 1M Levamisol; 20% Tween 20; 0.1M Tris-HCl) before adding NBT/BCP chromogen (Gibco, 1:380) to initiate staining. Staining proceeded until sufficient reaction was observed. Embryos were mounted in 80% glycerol and examined on a Zeiss Axioskop 2 microscope.

2.6 *In vitro* analysis

2.6.1 Plasmid constructs

The pPac3 basic vector, pPac3-*trh*, pPac3-*tgo*, pPac3-*ßgal* and the *btl* luciferase reporter construct pGL3-*btl* (P[B-123]) (Ohshiro and Saigo, 1997) were all provided by Dr. Woodgett (University of Toronto). Full-length JIGR1 and truncated JIGR1 without the MADF domain (JIGR1ΔMADF) were subcloned into the pPAC3 vector for *in vitro* expression (Sonnenfeld *et al.*, 2005). For full length JIGR1, the entire cDNA LD33329 sequence was copied through PCR as a *KpnI-XbaII* fragment for insertion and cloned in-frame with a C-terminal HA-tagged sequence. JIGR1ΔMADF was generated by PCR precisely like its full-length version but starting at sequence corresponding to amino acid

118. The amplified PCR fragments were first subcloned into a pCR 2.1-TA vector (Invitrogen) to optimize cloning and increase efficiency of restriction digestion. Digested PCR fragments were gel purified and ligated into the corresponding digested sites found in the gel extracted pPAC3 vector. T4 DNA ligase (New England Biolabs) was applied according to manufacturer instructions. 2.5 μl of ligation mixtures were used to transform *E. coli* DH5α cells (Invitrogen) and transformants were selected by plating on LB ampicillin medium. Pure cultures were prepared from selected transformants and plasmid DNA were isolated from these strains with plasmid minipreps (Qiagen) and analyzed by restriction digestion and DNA sequence analysis (Leal *et al.*, 2004).

2.6.2 Transfection of *Drosophila* cells

In order to experiment under *in vitro* conditions, *Drosophila* S2 cell cultures were used (Schneider, 1972). An insect cell specific transfection reagent, Cellfectin (Invitrogen), was used to introduce vectors containing desired sequences (2μg DNA/8μl Cellfectin) into the cells. Cells were handled in Schneider's *Drosophila* medium (Gibco) with 10% heat-inactivated fetal bovine serum (FBS) and Penicillin-Streptomycin (50 units penicillin G and 50 μg streptomycin sulfate per milliliter of medium). S2 cells were seeded in 6-well plates at a density of 10^6 cells per well at 27 °C and transfections were carried out in Schneider's medium sans serum and antibiotics according to Cellfectin manual instructions with various cDNA vectors.

2.6.3 Luciferase and β-galactosidase assays

Combinations of plasmids were added to the cells in the presence of pPac3-*βgal* and pGL3-*btl*. 48h after transfection cells were washed with 1X PBS. Triplicate samples were extracted with 200ul/well of 1X reporter lysis buffer (Promega). After one

30min freeze thaw cycle the cells were centrifuged (13000 rpm for 2min at 4 °C). Supernatant was collected and 30ul of each sample was added to 30ul of luciferase buffer composed luciferin (Invitrogen). Luciferase activity was measured by LMax II 348 (Molecular Devices, Sunnyvale CA) (absorbance at 595λ). The β-galactosidase activity was assayed by adding 30ul of sample to 200ul of β-galactosidase substrate buffer (1xPBS, 0.5mM MgSO4, 1.35ml of β-mercaptoethanol), 10% of 4mg/ml chlorophenolred-ß-D-galactopyranoside (CPRG; Calbiochem, San Diego, CA). Luciferase activity was normalized to β-galactosidase activity and plotted as the mean ± standard deviation of triplicates from a representative experiment.

2.6.4 S2 Immunohistochemistry

To determine the cellular localization of both full-length JIGR1 and JIGR1ΔMADF, S2 cells were transfected with pPAC3-*JIGR1* constructs described above. 48h post transfection, 250 µl of cells were seeded on chamber slides by centrifugation. Cells were fixed with 4% formaldehyde for 10min and washed with PBS. PBSB solution (PBS, 2% Triton-X-100, 0.5% BSA) washes followed to remove unspecific signals. Cells were incubated overnight at 4 °C with primary antibody rabbit anti-HA (Sigma) at 1:500 dilution. The next day, the primary antibody was removed with PBSB washes and cells were incubated with a FITC-conjugated secondary antibody (Jackson ImmunoResearch) for 1h at RT. Cells were repeatedly washed with PBSB. To label the nucleus, 0.4µl/ml DAPI was added for 2.5min. Samples were mounted in Vectashield medium (Vector Laboratories) and visualized with a Zeiss Axioskop 2 microscope.

2.6.5 Preparation of S2 cell lysates

Following transfection, the plates were washed in ice-cold 1X PBS and the cells were scraped for collection. To extract the protein, cells were incubated in RIPA lysis buffer (1% NP 40, 1% sodium deoxycholate, 0.1% SDS (w/v) 4.5 mM NaCl, 2.5 mM Tris (pH 7.4), 8 μM EDTA, 0.2 mM sodium phosphate (pH 7.2) with fresh, 0.5 mM PMSF, 1:100 protease inhibitor cocktail (Sigma), 1mM sodium pyrophosphate, 10 mM sodium fluoride and 100 μM sodium orthovanadate). The RIPA mixture was vortexed 3 times in a span of 20min to complete lysising. Supernatants were collected following a centrifugation at 10600 rpm for 5min at 4 °C. The concentrations of lysates were determined using Bradford reagents and a spectrophotometer.

2.7 JIGR1 protein

2.7.1 GST pull-down

A unique region of JIGR1 was PCR-amplified by using primers for the production of a pGEX-JIGR1 construct (pGEX-2T vector provided by D. Lohnes, University of Ottawa) this was produced and kindly provided by Xuetao Sun. The JIGR1 protein was prepared following the basic GST-fusion protein approach (Smith and Johnson, 1988). A 40 ml overnight culture was made and diluted into 4 L of LB medium the next day. When the culture reached a concentration of log phase A_{600} 0.6-0.8, Isopropyl β-D-1-thiogalactopyranoside (IPTG) was added to a final concentration of 0.5 mM and induced for 3h. Cell extracts were prepared first by centrifugation at 5,000 rpm for 10min and cell pellets were resuspended in 40ml cold 1X PBS. Cells were then lysated on ice by mild sonication after mixing with 1% Triton X-100. Finally, after another centrifugation

at 10,000 rpm for 20min, the supernatant was collected. A 2 ml bed volume of 50% glutathione slurry was made using Glutathione Sepharose 4B beads (Amersham Biosciences) mixed with 1X PBS at a 1.33X bed volume/ml ratio. The equilibrated 50% slurry was added to the culture supernatant and mixed at room temperature on a rocker for 30min. Following 3 washes with PBS, the beads were incubated for 10min and eluted three times with 1 ml elution buffer (10 mM Glutathione in 50 mM Tris-HCl; pH 8.0) per bed volume of Glutathione Sepharose 4B beads. Elutant was confirmed by sodium dodecyl sulfate polyacrylamide gel electrophoresis (SDS-PAGE) analysis, pooled and stored at -80 °C. A rabbit polyclonal JIGR1 antibody was generated by Cedarlane Labs, Burlington, ON using the purified GST-tagged protein as antigen.

2.7.2 Affinity purification

To prepare GST and GST-fusion protein columns, the protein was first coupled to CNBr activated-Sepharose Beads 4B (Amersham Biosciences), the eluted protein was first dialyzed in a coupling buffer (0.1M $NaHCO_3$; 0.5M NaCl; pH 8.3) overnight at 4 °C. The sepharose was prepared according to manufacturer's instructions in 1mM HCl. The prepared sepharose and dialyzed protein were mixed together at 4 °C overnight and incubated for another 6h at RT in a 0.1M Tris buffer. To complete the coupling, the resin was washed once in a 0.1M Acetate; pH 4.0/0.5 M NaCl solution, once in 0.1 M Tris-HCl pH 8.0/ 0.5 M NaCl solution and twice in 1X PBS. It is stored at 4 °C in PBS with 0.01% sodium azide. Another sepharose column was generated coupled to the GST protein in order to remove the anti-GST antibodies still tagged onto JIGR1 protein.

Anti-GST antibodies were removed first from serum (rabbit anti-JIGR1) by diluting 5 ml of serum with 5 ml of PBS/Tween (1X PBS; 0.2% Tween-20; 0.01%

sodium azide) and incubating it with 5ml of GST column in PBS/Tween for 2h at 4 °C. The sample was centrifuged for 1min to separate the supernatant which was collected for the subsequent incubation with GST-JIGR1 column to isolate anti-JIGR1 antibodies. The accumulated sample was incubated overnight at 4 °C with JIGR1 columns, after which the supernatant was removed and the remaining column was washed 5 times with 10ml PBS/Tween each and twice with PBS. The column beads were resuspended in PBS and transferred to a Bio-Rad column for elution. The protein was eluted with 10ml of 0.2 M Glycine (pH2.8) and collected in 700 µl aliquots delivered to Eppendorf tubes with 300 µl of 1M K_2HPO_4. Protein concentration was verified by Bradford Protein Assay (Pierce) and pooled for another overnight dialysis in PBS. The antibody was concentrated with Centricon tubes (Millipore) following manufacturer's protocol. Concentrated antibody was quantified and stored at -20 °C.

2.8 Generation of *UAS* lines for over-expression experiments

To determine the outcome of JIGR1 *in vivo* under gain-of-function conditions, the GAL4/UAS binary system method (Duffy, 2002) was chosen. Both UAS-*JIGR1*and UAS-*JIGR1ΔMADF* were subcloned into the pUAST vector (Sun *et al.*, 2006) as *KpnI-XbaI* fragments. The pCR-amplified fragments of both JIGR1 segments were cloned into pCR 2.1-TA shuttle vector, digested, gel extracted first before ligation into pUAST vector to increase quality of fully digested inserts. Cloned vectors were verified by sequencing and sent for injection to Genetics Services Inc., Sudbury, MA.

2.9 Primers

The following primers were used for all JIGR1 and JIGR1ΔMADF subcloning purposes with underlined base pairs indicating HA tag sequences:

JIGR1 full length

Forward:
5'CGT**GGTACC**ATGGAGAACCTGTCGCACTTGTATCCACCGCAGTTGCCAAA
3' KpnI

Reverse:
5'ATAT**TCTAGA**CCTAAGCGTAATCTGGAACATCGTATGGGTACTCGTCCTCC
TCCTG 3' XbaI

*JIGR1*ΔMADF

Forward:
5'**GGTACC**CCCAGGCGCAGCTTTAAGAACATGAGCGTAAAGGAGGAGGATGA
3' KpnI

Reverse:
5'ATAT**TCTAGA**CCTAAGCGTAATCTGGAACATCGTATGGGTACTCGTCCTCC
TCCTG 3' XbaI

RESULTS

3.1 *JIGR1* is located on chromosome 3R

JIGR1 (gene CG17383) is found on chromosome 3R at cytological region 96E6. The entire genomic region spans from 21463k to 21476k with the 5'UTR split over four regions and encompassing the majority of the introns in between each UTR region. The *JIGR1* gene is encoded by 8 exons interrupted by much shorter sequences of non-coding introns. The 3'UTR follows closely the last *JIGR1*coding region (Figure 7A). The closest neighbouring gene to *JIGR1* is *tankyrase*, a structural constituent of the cytoskeleton, located roughly 3 kb downstream (Flybase: http://flybase.bio.indiana.edu/).

Currently, there are 19 alleles of *JIGR1* obtained from various transgene insertions, three of these insertion lines were acquired for our studies of JIGR1 embryonic function. The main stock of flies used for all *JIGR1* related studies is EP(3)3354, located in front of the first 5'UTR region (Figure 7A). EP(3)3354 was obtained from Rørth's EP collection of flies which carry special *P* elements containing UAS binding sites (Blair, 2003). This promoter faces outward at the end(s) of the *P* element, so that when the *P* element is randomly mobilized throughout the genome, it activates the expression of nearby genes under the control of GAL4 (McGuire *et al.*, 2004). The other two lines, EY06847 and BG00794, also contain *P* element insertions and adhere to the same principles as EP lines. EY06847 is located 30bp downstream of the EP(3)3354 insertion, while the BG00794 insertion is located in the non-coding region of *JIGR1* between the second and third 5'UTR regions roughly 10kb downstream from EP(3)3354.

The translated full length JIGR1 is 336 aa in length and consists of one conserved domain called MADF (SMART: http://smart.embl-heidelberg.de/) that is 86aa long and

Figure 7. (A) Extended genomic region of JIGR1 (CG 17383). Located on the third chromosome between 21463kb and 21476kb. The 5'UTR is split over four different regions. The protein coding region of JIGR1 is found in three exons and directly before the 3 'UTR region. Three insertion elements are depicted to reflect the different JIGR1 lines tested in experiments. **(B) Translated JIGR1 protein.** Includes one conserved DNA binding domain, MADF, near the N terminus of the protein. **(C)** This truncated version of JIGR1 was used to make ΔMADF transgenes and as an antigen to generate a polyclonal antibody.

A

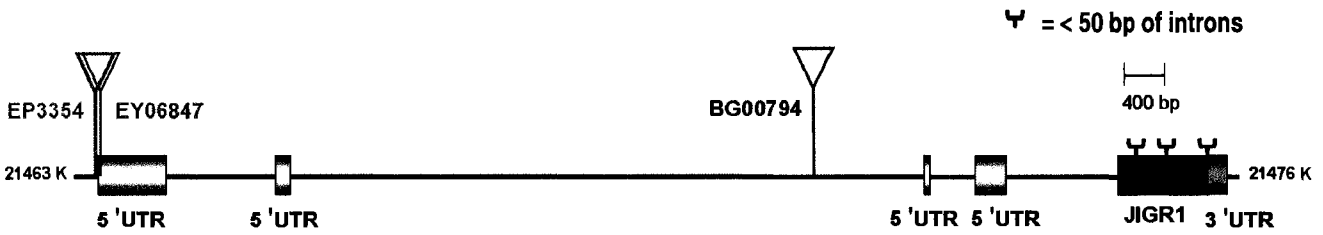
= < 50 bp of introns
400 bp
EP3354
EY06847
BG00794
21463 K
21476 K
5 'UTR
5 'UTR
5 'UTR
5 'UTR
JIGR1
3 'UTR

B

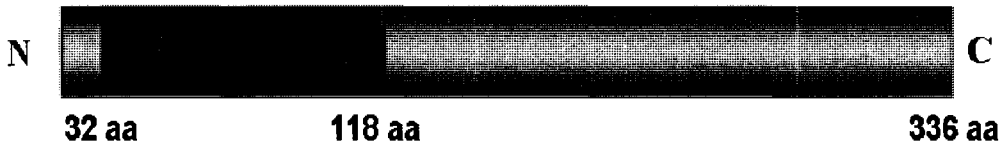
N
C
32 aa
118 aa
336 aa

C

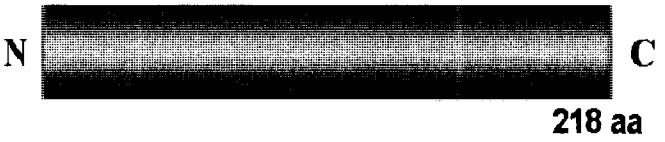
N
C
218 aa

located at the N-terminal end of JIGR1 (Figure 7B). A truncated ΔMADF JIGR1 protein was made from JIGR1 cDNA (LD33329, confirmed by sequence verification) to further isolate and examines the function of the MADF domain (Figure 7C). Truncated JIGR1 is 218aa in length and consist only of sequences found downstream of MADF.

3.2 MADF domain homology

In terms of function and purpose not very much is known about the MADF domain, but despite this lack of knowledge, the MADF domain is relatively prevalent and belongs to a large family of genes, especially in the genus *Drosophila*. A quick homology search on SMART (http://smart.embl-heidelberg.de) revealed 172 proteins containing this DNA-binding domain that specifically recognizes the sequence YAAC(G/T)G. 171 of the total proteins are found in eukaryotes plus one found in an undefined protein from *Amsacta moorei entomopoxvirus*. This is a well characterized insect poxvirus, primarily because it replicates in cultured insect cells (Marlow *et al.*, 1998). Of the 171 proteins, 81 are found in the Drosophilidae family and divided almost evenly between the *Drosophila melanogaster* and *Drosophila pseudoobscura* species, the larger half being in the former.

MADF sequences were also found in *Aedes aegypti* or more commonly known as the yellow fever mosquito, and possessing 19 uncharacterized proteins. MADF then skipped to another genus in the same family and 14 proteins were found in *Anopheles gambiae*. One other phylum of organisms that MADF repeatedly appeared in was the nematodes, 18 proteins were found over two genera of *Caenorhabditis*. The remaining MADF domains belonged to a wide spectrum of various organisms including yeast, a

flowering plant, sea urchins, sea squirt and recently 6 MADF domains were classified in another popular model organism, *Danio rerio*, also known as the zebrafish.

Curiously enough, none of the 42 other *melanogaster* proteins scored the highest in the BLAST search against *JIGR1* MADF, rather, the highest percentage identity of 71% and the highest percent of positive matches (similarity) of 82%, belonged to an uncharacterized protein (GA14496) in *Drosophila pseudoobscura* (Figure 8A). The *pseudoobscura* genome has been fully sequenced and often paired with the *melanogaster* genome for comparative genome sequence analysis. The two species diverged from each other approximately 21 to 46 million years ago (Stevison *et al.*, 2004).

As mentioned earlier, few MADF-containing proteins have been studied. One such protein is the *Drosophila melanogaster* Mes2, an essential transcription factor during larval development (Zimmermann *et al.*, 2006). Mes2 has the same domain organisation as *JIGR1* with its N-terminal MADF domain being almost the same size as JIGR1's, while the remainder of the protein is much longer than JIGR1. Mes2 and JIGR1 show 26% identity, and 42% similar aa in their MADF domains.

Another characterized *melanogaster* protein with a MADF domain is the transcription factor Adf-1. Its ubiquitous expression and recognition of specific sites in a diverse group of promoters establish the important role of Adf-1 in *Drosophila* biology (Cutler *et al.*, 1998). Adf-1 also has an N-terminal MADF domain while the remainder of the protein is slightly shorter than JIGR1. The MADF domain of Adf-1 is 34% identical and 53% similar to that of JIGR1.

Figure 8. JIGR1 MADF domain homology. (A) JIGR1 MADF has the highest homology to MADF gene in *D. pseudoobcura*. A total of 172 different proteins over a varied group of organisms contain the MADF domain. The majority of them being uncharacterized and predicted transcription factors. One such protein is GA14496 found in the *Drosophila* genus *pseudoobscura* which diverged from the *melanogaster* 21 to 46 million years ago. GA14496 MADF amino acid sequences had both the highest percentage identity and similarity at 71% and 82% respectively. Much higher score than any of the native MADF proteins found in *D. melanogaster*. **(B) JIGR1 MADF has similar domain length and organisation as MADF's found in transcription regulators Adf-1, Dip3 and Mes2.** Structurally, all the four proteins are very similar, with MADF domains that are about the same length. Nevertheless, their percentage identities and similarities are low to average at best when comparing MADF sequence homology. It is difficult to infer any similarities between them. All protein and domain structures were found using SMART (http://smart.embl-heidelberg.de/) and homology results were obtained from BLAST (http://www.ncbi.nlm.nih.gov/blast/Blast.cgi).

A

71% Identity, 82% Similarity

B

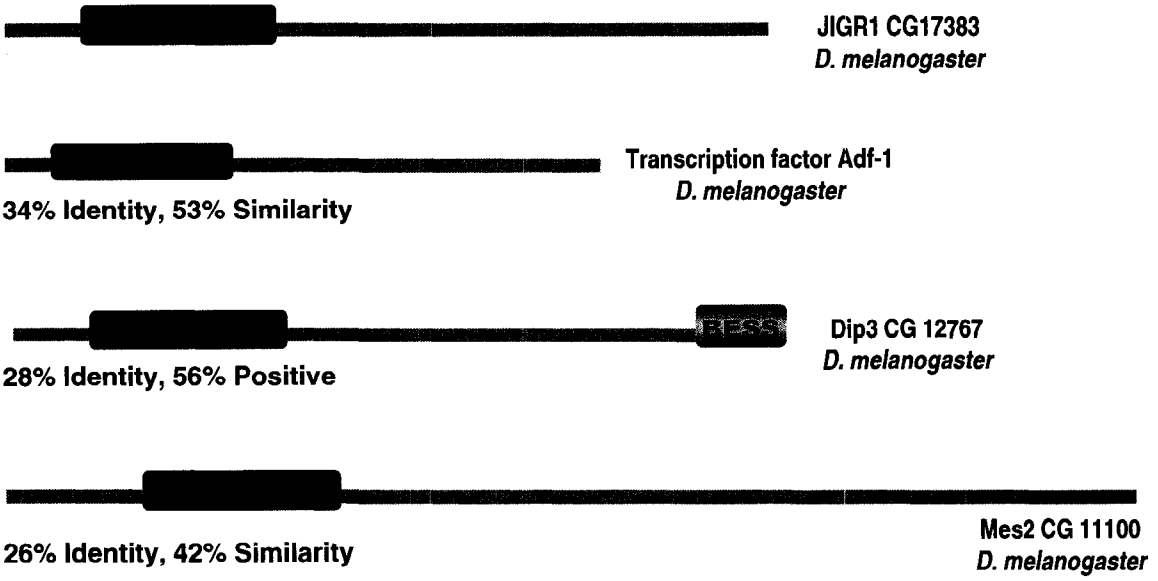

A third protein named Dip3 functions as a co-activator for the transcription factor Dorsal to regulate dorsoventral axis formation during *Drosophila* embryogenesis (Bhaskar and Courey, 2002). The MADF domain of Dip3 scored on the low side for both identity and positives, with 28% and 56% respectively, to that of JIGR1. In summary, it is difficult to infer homology between the MADF domain of JIGR1 and the MADF domains of Mes2, Dip3 and Adf-1 since their percentage identities are very low.

All protein and domain structures are found using SMART (http://smart.embl-heidelberg.de/) and homology results are from BLAST (http://www.ncbi.nlm.nih.gov/blast/Blast.cgi).

Therefore, MADF is an extensively observed protein conserved in many different families of species. Proteins with this domain all have the same domain organisation with little variation in domain length. Although *D. melanogaster* has 43 MADF-containing proteins, the MADF domain of JIGR1 shares the closest homology with its ortholog in *D. pseudoobscura* (Figure 8A).

3.3 *JIGR1* interacts synergistically with other *jing*-interacting genes in adults

The *Drosophila* eye is a focus of attention for defining mechanisms of development. Since the fly visual system is not required for survival of the organism, genetic manipulations specific to eye development are readily observable in the adult (Leiserson *et al.*, 1998). Studies over the past decade have utilized this system to gain insights into the cellular and molecular strategies regulating development (Pignoni *et al.*, 1997). A *jing* gain-of-function screen previously carried out in our laboratory identified seven additional genes that synergistically enhanced a rough eye phenotype indicating a

possibility of genetic interaction with *jing*. These uncharacterized genes, including *JIGR1* were referred to as *jing*-interactors. I decided to test the effects of over-expressing a few of *jing*-interactors: EP(3)625 (*DATR-X*), EP(3)3084, EP(3)3135, both independently and in synergy with *JIGR1* to determine if genetic interactions are present.

A wildtype compound eye contains an array of some 800 light sensing ommatidia or simple eyes. Each ommatidium comprises 8 photoreceptor neurons (R cells, designated R1–R8) arranged in organized clusters as shown by light microscopy (LM) (Figure 9B arrow) and as precise rows and columns (Figure 9A) as shown by SEM. Small mechanosensory bristles project from the anterior end of each facet in one uniform direction (Figure 9A, inset).

jing-interactors, EP(3)635, EP(3)3145, EP(3)3084 and EP(3)3354 (*JIGR1)* were first mis-expressed in the eye with *gmr-Gal4* individually. EP(3)635 had the least disruptions in eye development (Figure 9E and F), each ommatidium was still present in wildtype patterns and bristles on the facets were aligned in the correct orientation. However, the spaces between two ommatidia that are usually filled with secondary and tertiary pigment cells appear to be missing (arrow). Mis-expression of EP(3)3145 (Figure 9I and J) resulted in misalignment of R cells, and the presence of R8 (arrow), which under normal circumstances is not seen as it nestles between R1 and R2 in a more proximal plane. Unlike EP(3)635, the secondary and tertiary pigment cells do not appear to be missing, on the contrary, there seems to be an overgrowth in cells, possibly pushing the R cells out of position. At first glance the ommatidia of *gmr-Gal4*, EP(3)3084 look to be undisrupted, as all the R cells are developed in eye discs (Figure 9N), however, the secondary and tertiary pigment cells were replaced by vacuoles (Figure 9N, arrow). The

external morphology as viewed by SEM, showed that the overall eye was smaller and shrivelled in appearance; which may have been caused by the missing accessory cells. Bristle orientation was highly disorganized.

Mis-expression of JIGR1 (Figure 9C and D) gave rise to an entirely new phenotype of ommatidia. The number of R cells was still correct but no longer tightly clustered at the centre of each ommatidium. There was a slight rough eye phenotype visible by SEM (Figure 9C) and the bristles appear to be slightly disorientated.

When *JIGR1* was co-expressed with each of the other EP lines, synergistic effects on ommatidial development were observed (Figures. 9G, H, K, L, O and P). There were no signs of ommatidia and no recognizable R cells were found (Figures 9H, L and P). In ommatidia co-expressing JIGR1 and DATR-X, a few cell nuclei were present (Figure 9H, arrow), however, most of the tissue consisted of vacuoles. Ommatidia were not present after co-expression of JIGR1 with EP(3)3145 (Figure 9L) and EP(3)3084 (Figure 9P). Consequently, the corresponding SEM images showed a smooth appearance overlayed by disorientated bristles (Figure 9K and O).

Therefore, the R cell loss associated with the co-expression phenotypes was much more severe than the effects expected by simple addition of individual phenotypes which consisted only of pigment cell loss and ommatidia disorganization. In the eyes with loss of ommatidia, there is a possibility of cell apoptosis causing the death or a chance that the cells have never been specified during development.

Figure 9. *jing* interacting genes show synergistic interactions in the adult eye. Scanning and light microscopic analysis of eyes from adults expressing different genotypes under control of the *glass* promoter (P[*gmr-Gal4*]). **(A, B)** Heterozygous P[*gmr-Gal4*] flies have a wild-type arrangement of ommatidia (arrow) and mechanosensory bristles. **(C)** Expression of wild-type EP(3)3354 (*JIGR1*) in the eye causes a slight rough eye and the bristles appear to be less orderly. **(D)** In cross-sectional view, ommatidia are present but are not spaced properly. **(E and F)** Expression of EP(3)635 under GMR-*Gal4* control, does not affect eye development. **(G)** However, when JIGR1 is co-expressed with EP(3)635, the eye is badly deformed and appears to be shrunken. **(H)** The cross-section shows an absence of ommatidia and a replacement by empty vacuoles. **(I)** The SEM of EP(3)3145 expression presents an adult eye that appears wild-type. **(K, L)** Co-expression of JIGR1 and EP(3)3145 results in a lack of defined, individual ommatidium; the eye appears to be slightly shrunken in certain areas when viewed by SEM. Cross sections resemble that of JIGR1 and EP(3)635 co-expression. **(M)** Wild-type EP(3)3084 expression shows a strong disruption in the eye structure. **(O, P)** EP(3)3084 co-expressed with JIGR1 presents the most severe phenotype of all the crosses. **(P)** Ommatidia are not present and there are large empty vacuoles.

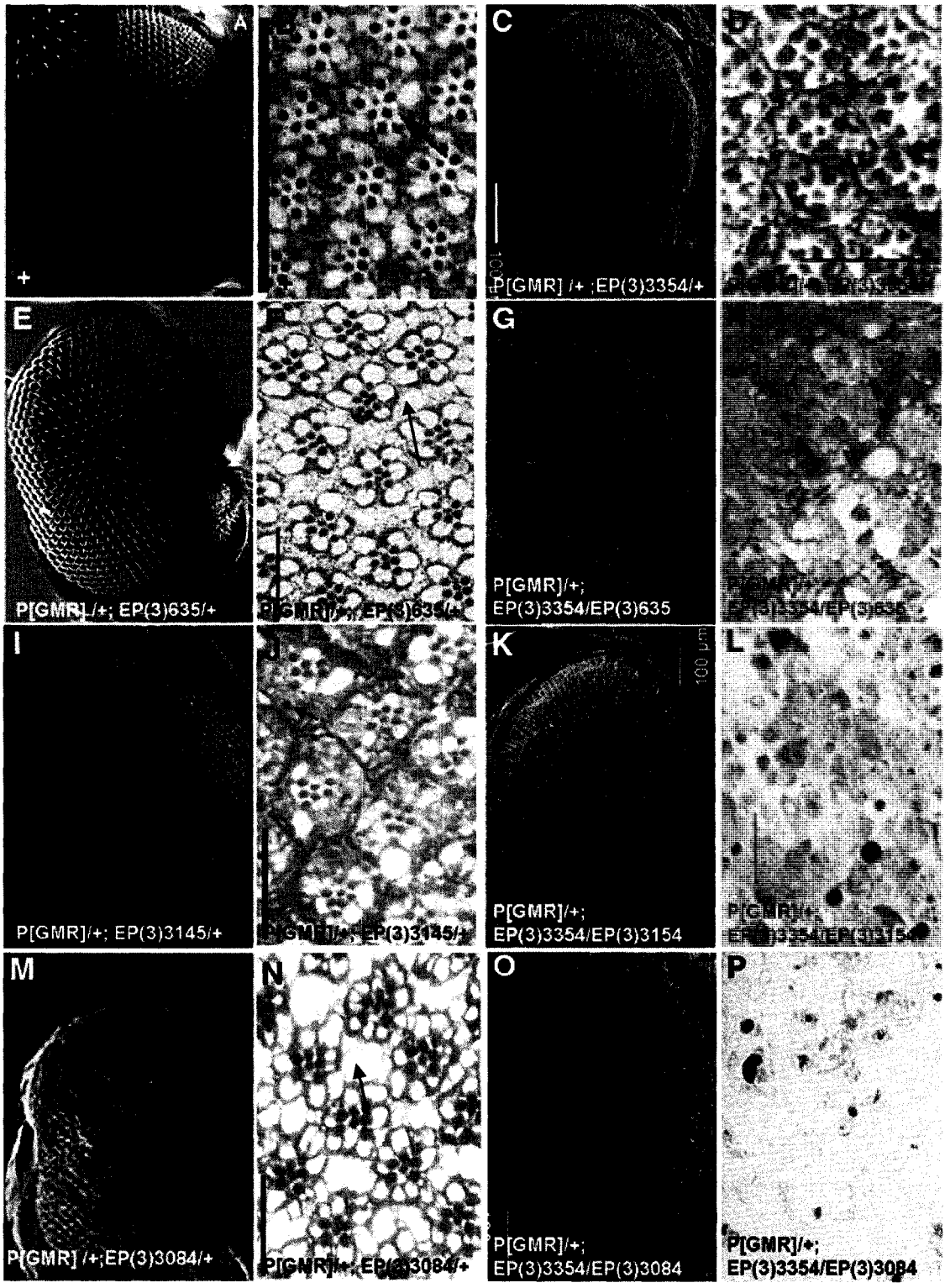
A
+
B
+
C
P[GMR] /+ ;EP(3)3354/+
D
E
P[GMR] /+; EP(3)635/+
F
G
P[GMR]/+;
EP(3)3354/EP(3)635
H
I
P[GMR]/+; EP(3)3145/+
J
K
P[GMR]/+;
EP(3)3354/EP(3)3154
L
M
P[GMR] /+;EP(3)3084/+
N
O
P[GMR]/+;
EP(3)3354/EP(3)3084
P
P[GMR]/+;
EP(3)3354/EP(3)3084

3.4 The JIGR1 protein is in the nucleus

To provide a more in-depth characterization of *JIGR1* and better understand the role of the MADF domain, I decided to determine the subcellular localization of JIGR1. Epitope-tagged full-length and MADF deleted JIGR1 were expressed in *Drosophila* S2 cells. To drive protein expression in S2 cells, full length pPAC-*JIGR1* and truncated pPAC-*JIGR1*ΔMADF constructs, both with C-terminal HA-tagged, were transfected into the cells using insect cell optimized transfection reagent, Cellfectin (Invitrogen). The cells were first stained with an anti-HA antibody and then with DAPI, a nuclear marker (Warren *et al.*, 2000). 100 cells were randomly selected from each set for analysis. In cells transfected with full length *JIGR1*, immunohistochemistry clearly shows a strong nuclear localization (Figure 10A, arrowhead) which corresponds and overlaps with DAPI staining after the images are merged. A few of the cells (19 %) did show what appears to be some cytoplasmic localization but not very strongly (arrow).

To test whether the MADF domain plays a role in JIGR1 subcellular localization, immunostainings for anti-HA were analyzed in S2 cells transfected with *JIGR1*ΔMADF-HA. Like full length JIGR1, the truncated protein predominantly localized to the nucleus in all cells (Figure 10D, arrowhead) however more cytoplasmic protein was now detected. Nearly all the cells (97%) had JIGR1ΔMADF activity outside the nucleus (arrow). When viewed under merged conditions, it is evident that the majority of the protein was found inside the nucleus but the presence of anti-HA immunoreactivity in the cytoplasm was clear (Figure 10F, arrow). Both full length and truncated transfection and immunostainings were repeated three more times and identical phenotypes were seen each time.

Figure 10. JIGR1 is present in the nucleus of *Drosophila* S2 cells. A Haemagglutinin (HA)-tagged full-length and truncated JIGR1 were expressed in S2 cells. The cells were treated with an anti-HA antibody followed by DAPI, a nuclear marker. **(A)** Full-length HA-JIGR1 is predominantly expressed in the nucleus (arrowhead), while low levels are present in the cytoplasm (arrow). **(B)** Same cells were treated with DAPI and merged **(C)** for nuclear confirmation. **(E-G)** HA-JIGR1ΔMADF is also predominant in S2 cell nuclei. Arrows in **(E)** reveal more cytoplasmic localization **(F)** once again confirms nuclear localization. Experiments were repeated three times.

JIGR1

JIGR1ΔMADF

There are many potential explanations for the differential localization of anti-HA in JIGR1 versus *JIGR1*ΔMADF transfected insect cells. For example, if JIGR1 requires the MADF domain to bind DNA, then in its absence the protein may not be retained as well in the nucleus.

3.5 Generation of polyclonal JIGR1 antibody

A polyclonal JIGR1 antibody was raised against the non-conserved region (402b to 1011b) of the original cDNA (LD3329, BDGP) to avoid cross-reactivity with other *Drosophila* MADF-containing proteins. The protein was produced from a pGEX-JIGR1 vector (provided by Xuetao Sun) according to the protocol described for GST-fusion protein purification by Smith and Johnson (Smith and Johnson, 1988). JIGR1 protein was further isolated by using Glutathione Sepharose 4B beads. The size of the GST-JIGR1 elutant was confirmed by SDS-PAGE analysis (Figure 13C) before sending away for production of a rabbit polyclonal antibody. Usually, the protein is cleaved with *thrombin* enzyme first to remove GST sequences and verify protein size, but in this case GST and JIGR1 proteins were almost equal in size (~25 kD and 27kD). Therefore, GST-JIGR1 was used as antigen for antibody production and GST proteins were removed from serum.

Affinity purifications were carried out on anti-JIGR1 serum to remove residual anti-GST antibodies and any other non-specifics present in the serum. Sepharose columns coupled with the desired target protein were generated (see Materials and Methods). A final concentration of 0.8mg/ml of purified anti-JIGR1 was collected and stored at -20 °C. Specificity of the antibody was first confirmed in flies ectopically

expressing JIGR1 (*prd*-Gal4/EP(3)3354 flies) by searching for the unique pair-rule pattern of segmentally repeating stripes (Figure 11A and B arrow).

3.6 Distribution of JIGR1 in the developing embryo

Where JIGR1 is localized provides many clues to the role JIGR1 plays during embryogenesis. Immunohistochemistry was carried out on multiple stages of Drosophila embryos using anti-JIGR1. Embryos were collected from control flies (w^{118}) on apple-juice agar plates at 25 °C every 6 hours and overnight. These multi-staged embryos were fixed in 4% formaldehyde and incubated overnight in a 1:500 dilution of anti-JIGR1. FITC-conjugated secondary antibodies (Jackson ImmunoResearch) and confocal microscopy were used to determine the distribution of JIGR1 protein throughout embryogenesis.

High levels of JIGR1 protein were detected in blastoderm embryos, 2h after egg laying (AEL), revealing that JIGR1 is present before the start of zygotic transcription and was acquired from maternal mRNA. JIGR1 is widespread during gastrulation (~3h AEL) and predominant in the cephalic furrow (Figure 11D arrow). When the embryo reaches stage 11 (4h AEL) parasegmental furrows (psf) that subdivide the germ band into metameric units appear (Figure 11E arrow) (Hartenstein, 1993;Sonnenfeld *et al.*, 2005). Figure 11E demonstrates that high levels of JIGR1 were accumulated in the ectoderm and was as ubiquitously expressed as before.

During the final stages of embyogenesis, 16 and 17 (~10h AEL), JIGR1 is present in the ectodermal cells overlying the ventral nerve cord (VNC) as well as throughout the VNC itself. Within the VNC, JIGR1 is present in the lateral CNS (Figure 11F arrow) and

Figure 11. JIGR1 protein localization during embryogensis. Fluorescence microscopy of a polyclonal JIGR1 antibody raised to the C-terminal 218 amino acids of JIGR1. Shown are 1μm merged stacks taken at 40x (NAOS) magnification with anterior to the left. Frontal images of the ventral side of the embryo **(D, F, G)**. Sagittal views with ventral down **(A, B, C, H)**. Dorsal view **(E, E1)**. **(F, G, H)** The same embryo in different planes of view. **(A and B arrows)** Segmentally repeating pair-rule stripes found in *prd-Gal4*/EP(3)3354 flies to confirm the specificity of anti-JIGR1. **(C)** A blastula stage embryo (2 hrs AEL) showing the presence of high levels of JIGR1 protein ubiquitously distributed. **(D)** A gastrula embryo showing ubiquitously distributed JIGR1. **(E)** At stage 11, parasegmental furrows (psf) (arrow) subdivide the germ band into metameric units. High levels of JIGR1 are present in the ectoderm throughout each parasegment. **(E_1)** A closer view of individual cells from panel **(E)**. **(F, G and H)** During the final stages of embryogenesis, more defined structures have relatively higher JIGR1 levels as compared with the surrounding ectoderm. **(F)** Arrow and arrowhead point to JIGR1 expression in the cells surrounding the axon scaffold (lateral CNS) and within the midline, respectively. In a more ventral view **(G)** JIGR1 is still clearly ectodermal. In sagittal view **(H)**, JIGR1 was intensely expressed in the peripheral nervous system (PNS). Arrows denote PNS sensilla.

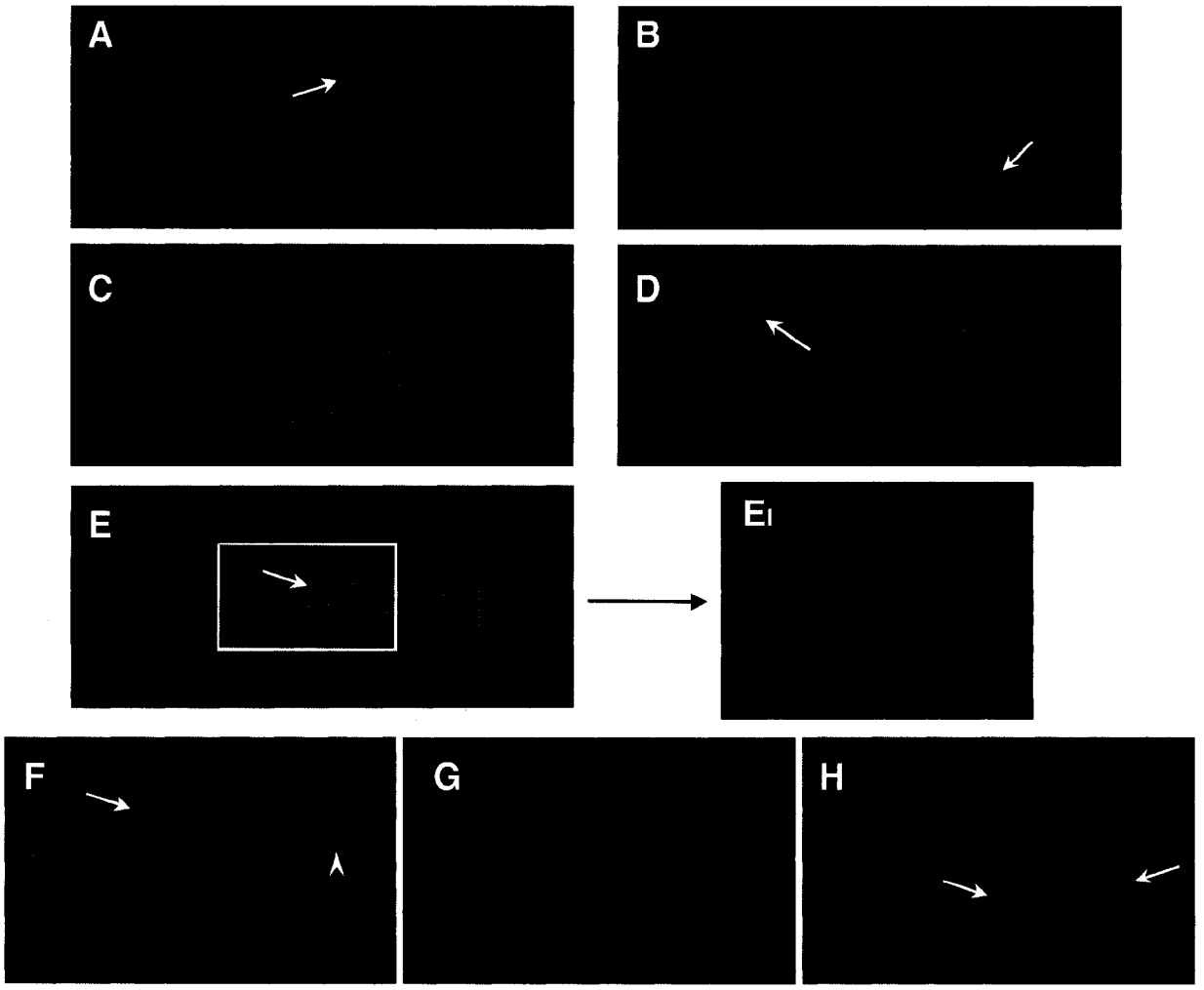
A
B
C
D
E
EI
F
G
H

in the cells at or near the midline (Figure 11F arrowhead). Another interesting discovery made in the older stages of development was that when examining the embryo in sagittal view, JIGR1 was present at relatively higher levels in the peripheral nervous system (PNS) as represented by the differentiated PNS sensilla (Figure 11H arrows). Recent unpublished data obtained from the Sonnenfeld lab have confirmed these results through double labelling the PNS with antibody 22C10 and anti-Fasciclin. The PNS stainings correspond perfectly with anti-JIGR1 immunostaining.

3.7 JIGR1 probe detects mRNA expression in the CNS and brain

The expression pattern of JIGR1 mRNA was determined by *in situ* hybridization to whole-mount embryos (see Materials and Methods). A JIGR1 digoxigenin-labelled RNA probe was first tested for its ability to identify JIGR1 mRNA when ectopically induced. The driver line *prd-Gal4* expresses the reporter gene in a paired-like pattern; Figure 12A and B are the lateral and ventral views, respectively, of pair-rule embryos carrying both *prd-gal4* and EP(3)3354. The probe only hybridized to paired stripes (arrows), providing evidence that it is specific to JIGR1 and at the same time confirming that the EP(3)3354 line induces JIGR1 expression.

In wildtype embryos, stage 11-12, expression was detected in the developing CNS. The embryonic CNS comprises the brain and segmented ventral nerve cord which derive from the neuroectoderm (Uhler *et al.*, 2002). All three corresponding elements were seen with the hybridization. Since the precursor neuroblasts are developed from the neuroectoderm, JIGR1 could have active roles in both early neurogenesis and further differentiation of cells in the CNS including the embryonic brain.

Figure 12. JIGR1 is actively expressed in CNS development. Whole mount *in situ* hybridization was performed using DIG-labelled riboprobes of *JIGR1* cDNA at stage 12, gastrulation, of development. **(A and B)** lateral and ventral view depicting the paired-patterns unique to *prd-Gal4/*EP(3)3354 to confirm probe specificity. **(C and D)** Sense probe controls. **(E and F)** *JIGR1* mRNA transcripts expression in wildtype w^{118} embryos at the gastrulation stage. The lateral view depicts active transcripts in both the neuroectoderm (arrow) and the brain (arrowhead), while the ventral view shows the ventral nerve cord (arrow). **(G and H)** Homozygous *Df(3R)Exel6203* embryos with deficient region covering JIGR1 locus.

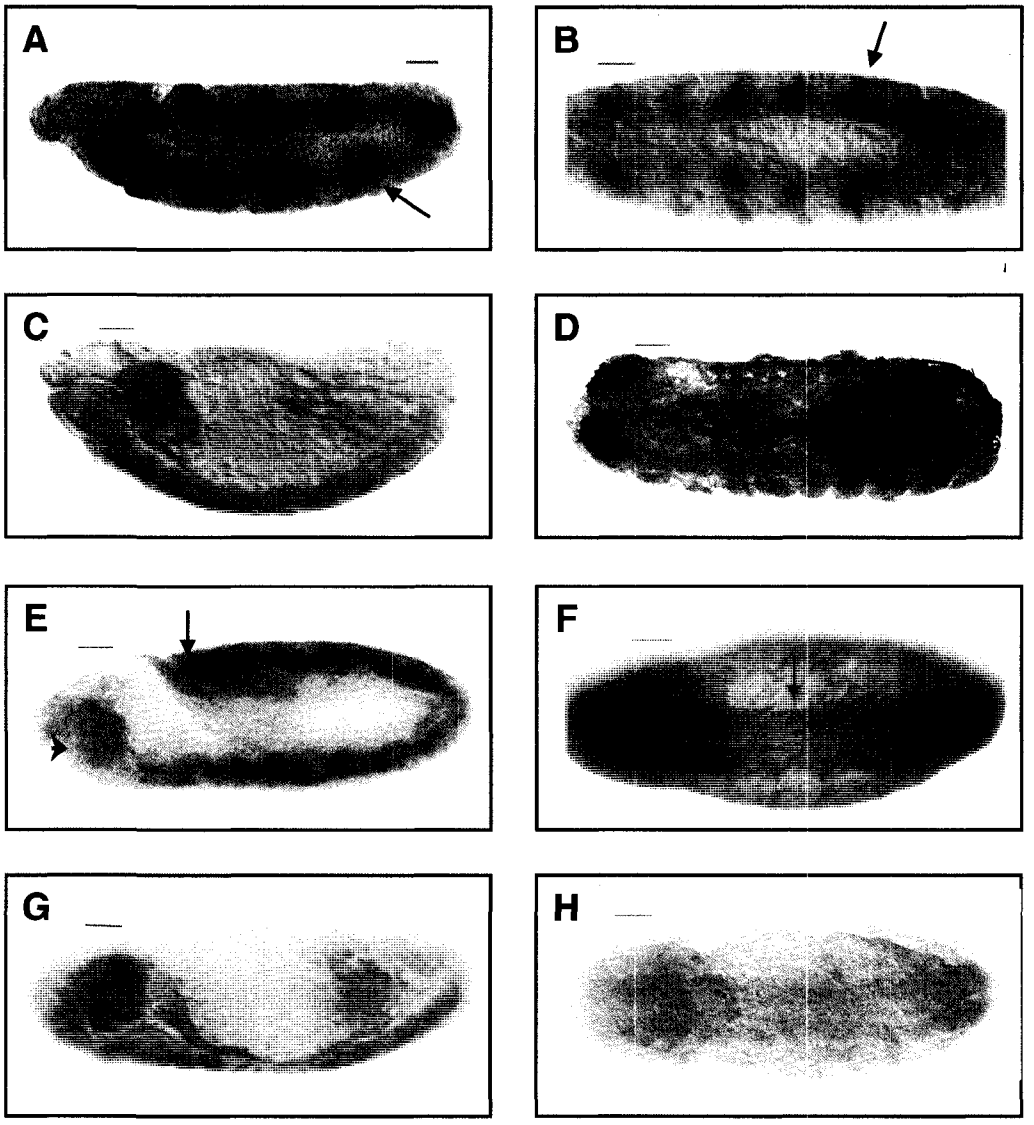
A
B
C
D
E
F
G
H

3.8 Generation of *in vitro* and *in vivo* expression constructs

In order to introduce JIGR1 protein into cells and embryos via injection, *JIGR1* must first be sub-cloned into different expression vectors for transcription and delivery purposes. Vectors were also required to generate truncated JIGR1ΔMADF proteins. To over-express *JIGR1 in vivo*, full length and truncated *JIGR1* were subcloned in-frame into a pUAST vector. The pUAST vector is commonly used for GAL4-mediated expression of exogenous genes, because it contains five *UAS* elements which bind Gal4, an *hsp70* transcriptional start site, and a multiple cloning site (Rorth, 1998). For *in vitro* expression, JIGR1 constructs subcloned into the pPAC vector, a *Drosophila* actin 5C promoter-driven expression vector (Ikeda *et al.*, 2001).

For both vectors, primers were designed to insert JIGR1 cDNAs at the *KpnI* and *XbalI* location within each of their respective multiple cloning sites. Both full length and truncated *JIGR1* constructs were designed with an HA tag at the C-terminus of the gene for double labelling purposes. For full length JIGR1, primers encompass the entire 1011bp of *JIGR1* cDNA, while primers for JIGR1ΔMADF amplify only the C-terminal 657bp.

Once the sequences were cloned into the desired vectors, they were cleaved with the same pair of restriction enzymes used for ligaton to verify insert by length (Figure 13A and B). Once confirmed, the newly cloned vectors were sequenced before injection in *Drosophila* embryos or transfection into S2 cells.

Figure 13. Confirmation of various *JIGR1* full length and *JIGR1*ΔMADF plasmid constructs. **(A)** For future misexppresion analyses, full-length and MADF-truncated JIGR1 constructs were subcloned into a pUAST vector generating UAS-*JIGR1* and UAS-*JIGR1*ΔMADF. Both constructs were generated by subcloning into the *KpnI* and *XballI* sites of the pUAST vector and were digested with the same enzyme pair to verify inserts. **(B)** JIGR1 and JIGR1ΔMADF were subcloned into the pPAC3 vector for expression in *Drosophila* S2 cell lines. Shown are *KpnI* and *XbaI* restriction enzyme digests to release the 1.0kb JIGR1 and 0.65 kb JIGR1ΔMADF inserts from pPAC. **(C)** A GST-JIGR1 fusion protein on SDS-Page gel for protein detection and quantification.

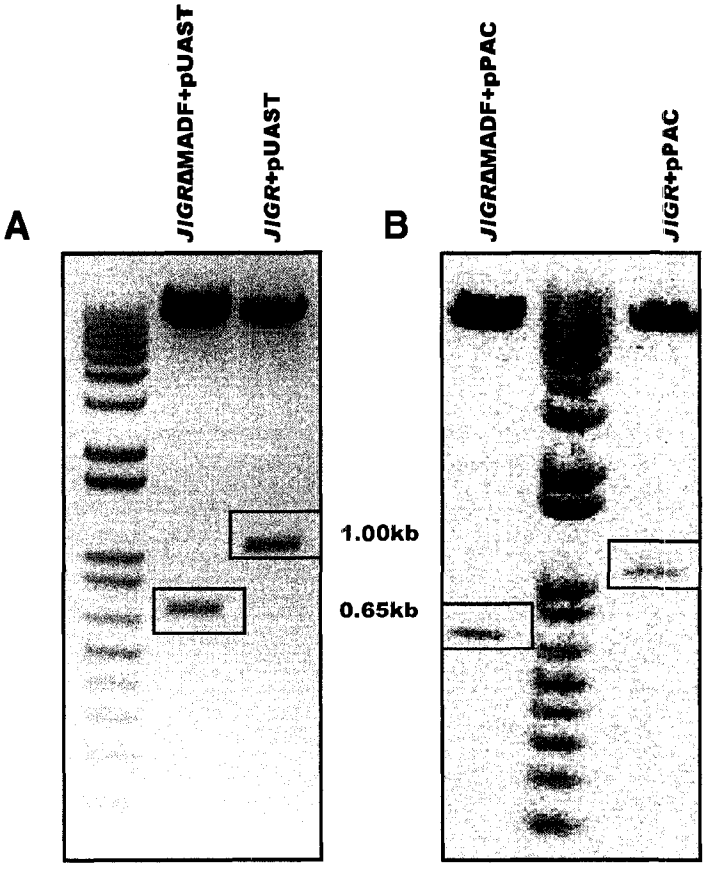
A
JIGRΔMADF+pUAST
JIGR+pUAST
1.00kb
0.65kb
B
JIGRΔMADF+pPAC
JIGR+pPAC

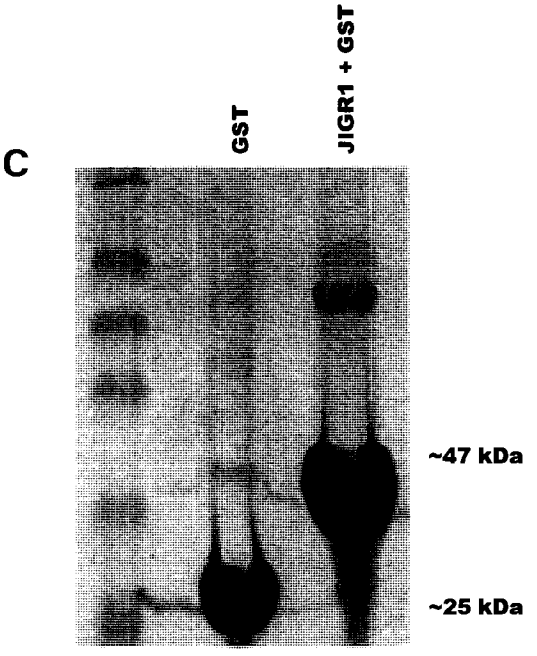
C
GST
JIGR1 + GST
~47 kDa
~25 kDa

3.9 *JIGR1* expression levels in glia are important for CNS axon formation

To determine if there are JIGR1 gene dosage effects in the CNS, phenotypes associated with over-expression of *JIGR1* and with embryos homozygous for a deficiency covering the *JIGR1* locus were analyzed. The GAL4/UAS system was once again used to over-express *JIGR1* in all CNS glia. Flies containing *gcm-Gal4*, a glial cell driver (Freeman *et al.*, 2003), were crossed to the *JIGR1* driving line, EP(3)3354, and their progeny were stained with BP102 to assess CNS axon formation which are directed by glial cells (Hidalgo *et al.*, 1995). *Df(3R)Exel6203* flies were used for *JIGR1*deficiency purposes, it lacks region 96E2-96E6 of the third chromosome where *JIGR1* is found. $jing^3$, a lethal ethylmethane sulfonate (EMS)-induced *jing* mutation, was used for *jing* deficiency studies (Sedaghat *et al.*, 2002).

In control flies, wildtype glia cells direct the commissures and longitudinal tracts to form a rectangular axon scaffold in each segment (Figure 14A). Mis-expression of one copy of EP(3)3354 in the CNS glia was associated with improper commissural and longitudinal axon formation (Figure 14B). The anterior and posterior segmental commissures (arrowheads) were not properly separated and there was a thinning of the longitudinal axon tracts connecting consecutive segments (arrows). Embryos homozygous deficient for *JIGR1* had fused commissures as well, and thin longitudinal axons (Figure 14C). An absence of longitudinal axons was also observed in *Df(3R)Exel6203/Df(3R)Exel6203* embryos (Figure 14C arrows).

In embryos heterozygous for $jing^3$ or *Df(3R)Exel6203* CNS axon tracts formed properly (Figure 14E). However, in embryos double heterozygous for both $jing^3$ and *Df(3R)Exel6203*, there was a thinning and loss of longitudinal connectives and a fusion of

anterior and posterior commissures (Figure 14D). Therefore, the combined dosage of *jing* and a gene(s) within *Df(3R)Exel6203* (possibly *JIGR1*) is critical for proper CNS axon development. This does not, however, indicate whether the two genes function in the same pathway or in parallel pathways from each other.

With *in vivo* studies, it is difficult to assess the degree of severity between samples due to the large variability in axon phenotypes. One way to measure strength of defects is by determining the expressivity of axon defects. Expressivity measures the degree to which a phenotype is expressed. The percentage of defective segments per embryo was determined for genotype including *gcm*-Gal4/EP(3)3354, *Df(3R)Exel6203/jing*^{3}, *Df(3R)Exel6203/Df(3R)Exel6203* and the heterozygote controls (Figure 14E). A minimum sample size of 680 segments was counted.

95% of segments in the ventral nerve cord of embryos homozygous for *Df(3R)Exel6203* showed either commissural or longitudinal defects, while only 3% of *Df(3R)Exel6203* heterozygotes had axon defects (Figure 14E). Embryos heterozygous for *jing*^{3} and Df(3R)Exel6203 showed 55% of segments defective for axon tract formation. This reveals that *jing*^{3} and *Df(3R)Exel6203* show strong gene dosage effects in the CNS.

Expressing high levels of JIGR1 in all CNS glia (*gcm*-Gal4/EP(3)3354) was associated with an 86% expressivity of axon defects.

Figure 14. JIGR1 glial function is required for axon pathfinding. Embryos stained with BP102 to analyze the over-expression and loss-of-function phenotypes of JIGR1. **(B)** JIGR1 over-expression in CNS glia using glial cells missing (GCM) driver is associated with defective longitudinal and commissural axon formation as compared with wild-type **(A)**. **(C and D)** Homozygous deficient embryos and those in trans to the *jing*^{3} mutation disrupt axon development. Arrows denote loss of longitudinal axons and arrowheads point to loss of differentiated commissures. **(E)** Percentage expressivity of axon defects per defective embryo for each line was collected to compare degree of severity. Controls consisting of *JIGR1/w*^{118} and *jing3/w*^{118} were counted.

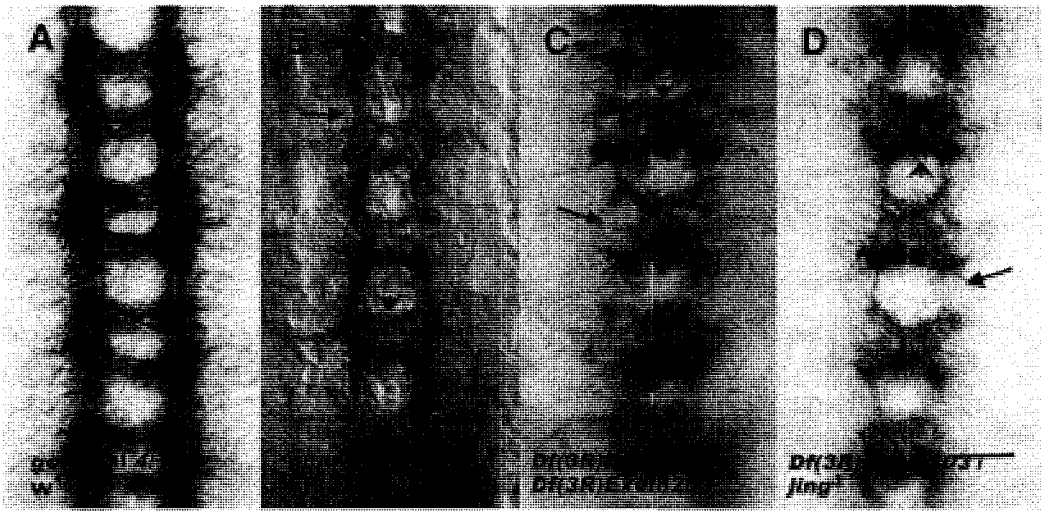
A
C
D

E

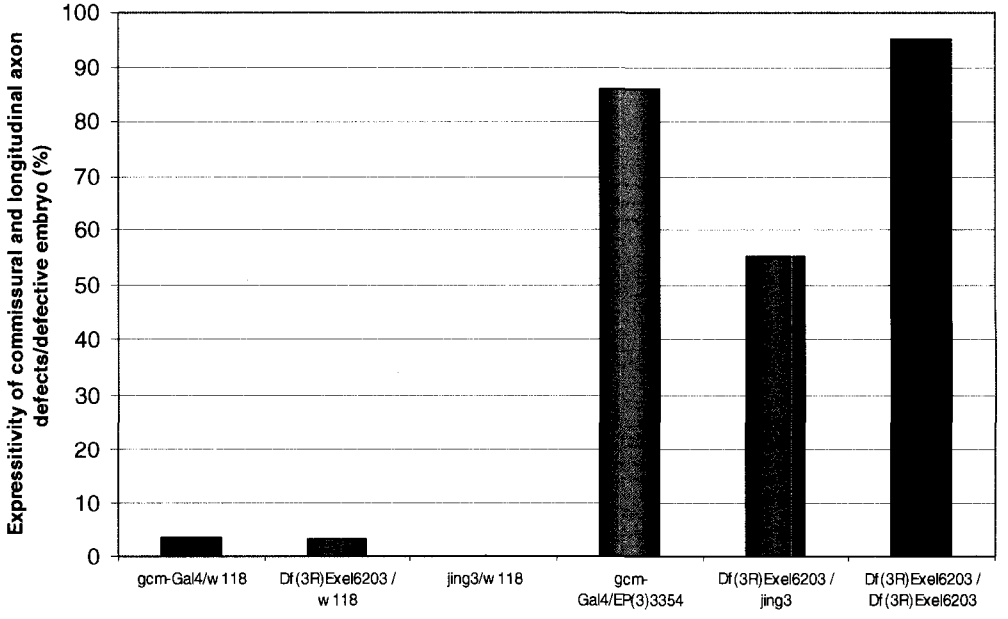
Expressitivity of commissural and longitudinal axon defects/defective embryo (%)
100
90
80
70
60
50
40
30
20
10
0
gcm-Gal4/w 118
Df(3R)Exel6203 / w 118
jing3/w 118
gcm-Gal4/EP(3)3354
Df(3R)Exel6203 / jing3
Df(3R)Exel6203 / Df(3R)Exel6203

3.10 *JIGR1* affects tracheal tubule formation

After discovering *jing* is involved in tracheal patterning (Sedaghat *et al.*, 2002), I wanted to determine *JIGR1* dosage affects in tracheal development. Loss-of-function was determined by examining embryos that are missing the *JIGR1* containing region of the 3R chromosome and JIGR1 gain-of-function embryos were generated by crossing flies carrying the *btl-Gal4* driver with those carrying EP(3)3354. Their progeny were stained with monoclonal 2A12 antibody which conveniently selects for tracheal lumen (Han *et al.*, 2004).

Figure 15A depicts a wildtype tracheal tree at stage 14 of development. The dorsal branches of all segments have fused into the dorsal longitudinal tracheal trunk (arrow) and transverse connectives are developed (arrowhead). Embryos homozygous for *Df(3R)Exel6203* are associated with breakages in the dorsal trunk (arrows) and losses of transverse connectives and the lack of a visceral branch (Figure 15B). Very similar results were observed in embryos expressing high levels of JIGR1 specifically in the trachea. Therefore, tracheal formation is highly dose-sensitive to *JIGR1*, any increase or decrease in gene quantity will result in a failure in tracheal tubule development.

3.11 JIGR1 has no effect on Trh::Tgo-mediated transcription of btl-Luciferase promoter

It has been proposed that *jing* co-operates with Trh::Tgo heterodimer in activation of *btl* gene *in vitro* (Sedaghat *et al.*, 2002). Since the discovery of genetic interaction between *JIGR1* and *jing* in the initial GOF screen, *JIGR1* could possibly regulate *btl* in the same pathway. The ability of *JIGR1* to transactivate Trh::Tgo mediated transcription of

btl was tested by transient transfections and luciferase assays performed on S2 cells by using Cellfectin (Invitrogen) according to manucfacturer's specifications. A reporter construct containing the minimal promoter of the *btl* (pGL3-*btl*) gene which includes three Trh::Tgo DNA binding sites (CMEs) was used because it is known to be activated by Trh::Tgo heterodimers (Ohshiro and Saigo, 1997;Sonnenfeld *et al.*, 2005). All transfection and luciferase assays were carried out in triplicates and repeated twice more in order to collect three sets of data for each experimental line. Statistical significances were calculated with a Student's *t* test.

When S2 cells carrying pGL3-*btl* were co-transfected with *trh* and *tgo*, transcriptional activities increased to 3-fold above control levels (Figure 16). First, pPAC-*jing* was added to the transfectant cocktail to define *jing*'s role in the transcription of *btl*. Unlike expected, there was a significant decrease in transactivation activity ($P < 0.05$), seemingly as if the addition of *jing* has down-regulated Trh::Tgo activation abilities. Comparable results were seen with the addition of *JIGR1*. Even when *jing* and *JIGR1* were co-transfected together no additive effects were seen. For this *in vitro* assay with a *btl* promoter region that contains three CME's, both *jing* and *JIGR1* did not favour Trh::Tgo transactivation.

Figure 15. JIGR1 dosage is important for tracheal tubule formation. Stage 14 embryos were stained with monoclonal 2A12 to identify tracheal tubules. Embryos are shown in sagittal view with anterior to the left. **(A)** Describe wildtype trachea. **(B)** Tracheal tubules are broken **(arrow)** in *Df(3R)Exel6203* homozygous embryos. **(C)** EP(3)3354 expression was directed to the trachea with the *btl*-Gal4 driver. High levels of JIGR1 in the trachea are associated with breaks in the tubules **(arrow)**.

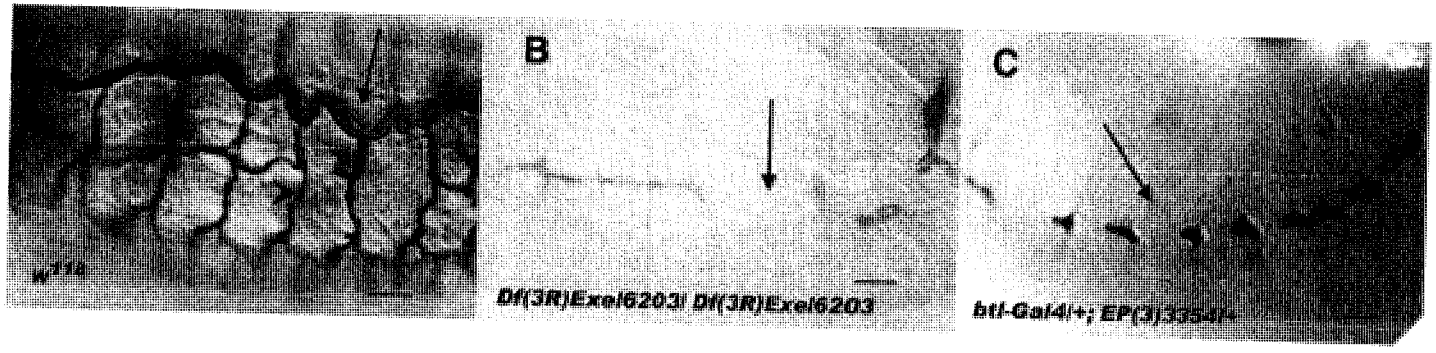
B
C
Df(3R)Exel6203/ Df(3R)Exel6203
btl-Gal4/+; EP(3)3354/+

Figure 16. JIGR1 and Jing reduce Trh::Tgo-mediated activation of a *btl*-Luciferase reporter in *Drosophila* S2 cells. Samples containing different combinations of JIGR1 and Trh::Tgo were tested on the *btl* promoter (pGL3-*btl*). S2 cells were co-transfected with Trh, Tgo and full length JIGR1 using Cellfectin transfection reagent. The capacity of Jing to induce transcription activation of *btl* and interaction between Jing and JIGR1 on the promoter were also tested. Transfection efficiencies were normalized using a ßgal expression plasmid, pPAC-ßal. JIGR1 had no additive effects and appeared to reduce Trh::Tgo-mediated *btl*-Luciferase activity. Experimental data was obtained as an average of best of two in three repeats for each sample. Error bars display standard deviation of the averages obtained. Statistical significances were determined with a Student t-test.

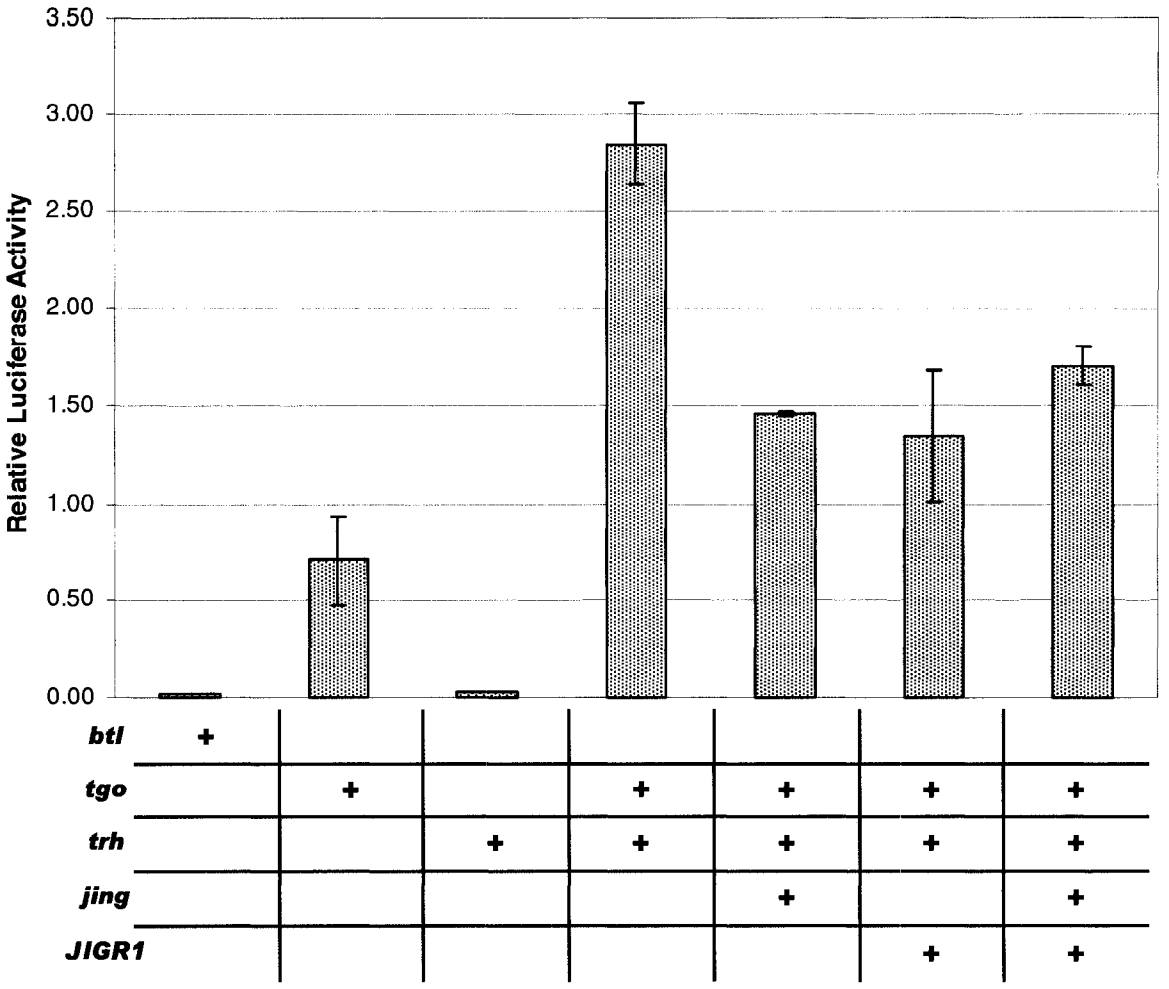
Relative Luciferase Activity
3.50
3.00
2.50
2.00
1.50
1.00
0.50
0.00
btl
tgo
trh
jing
JIGR1

DISCUSSION

4.1 MADF: large gene family with weak homology

It is of significant importance to ascertain the potential role of the MADF domain as it is the only identifiable region *JIGR1*. There exists a large MADF domain-containing gene family. Despite the majority being uncharacterized, of the few genes that were characterized, all had MADF domains that functioned in gene transcription regulation (Cutler *et al.*, 1998;Bhaskar and Courey, 2002;Zimmermann *et al.*, 2006). The MADF domain has been identified in a variety of organisms, including flies, worms, sea urchins and fish. Presently, there is no trace of this domain observed in mammalian genomes. In certain MADF organisms, such as *Drosophila melanogaster*, there are prevalent occurrences of this domain, but the sequence similarities are very weak and are most probably unrelated. Save for the one MADF sequence found in *Drosophila pseudoobscura* (GA14496), not many residues are conserved among all the family members in other organisms. Therefore, if the sequences were indeed related, which seem doubtful, they are too distant to be properly assessed for homology. Furthermore, given the presence of MADF in vertebrates such as the zebrafish, but a complete lack of it in mammalian genomes, makes this pattern of evolutionary conservation unique, if it so should exist.

It is very likely gene GA14496 in *D. pseudoobscura*, which scored the highest percent identity to our MADF, is an ortholog for *JIGR1*. The genome for *D. pseudoobscura* has been fully sequenced and systematically compared to *D. melanogaster*'s genome. 12,179 regions of the *D. pseudoobscura* genome contain a putative ortholog of a *D. melanogaster* gene; the majority of these ortholog protein sequences show >70% amino acid identity (Richards et al., 2005), this concurs with our

results of a protein identity level at 71%. Unfortunately, the functions of the gene in *D. pseudoobscura* have yet to be established and cannot provide further clues as to the role of the MADF domain in JIGR1.

Although there is no refuting the necessity of the MADF domains studied in the three proteins, their low scoring identities makes them disadvantageous candidates for deducing possible functions for the MADF domain of JIGR1. However, the significance in their similarities should not be overlooked because of their modest homology. Apart from their domain organisation and size, loss-of-function assays of *mes2, adf-1* and *dip3* revealed they each play essential roles as transcription activators or coactivators for proper *Drosophila* embryogenesis. This is largely due to their DNA binding MADF domains (Cutler *et al.*, 1998;Bhaskar and Courey, 2002;Zimmermann *et al.*, 2006). Homology between the three is also humble, but certain sequence motifs still resemble one another. One such motif is the 3-nucleotide pyrimidine-rich repeats found in Adf-1 MADF, it is reminiscent of the 3-nucleotide repeats motif of a pair of pyrimidines followed by either an adenine or thymine found in Dip3 MADF (Bhaskar and Courey, 2002).

In conclusion, based on the trend seen in the previously characterized MADF proteins, it is possible that the JIGR1 MADF domain is more related to other MADF domains in function and purpose than in sequences structure. A closer inspection of its DNA binding abilities and determining the actual binding sequences of JIGR1 MADF should fill in more pieces of the puzzle. Of course, comparative genome sequencing is a powerful tool in the ongoing effort to annotate and analyze genes. The *D. pseudoobscura* gene GA14496 should be inspected for other possible parallels, such as relative embryo

localization and perhaps interactions with *jing* and *jing*-interactor homologs found in its genome.

4.2 *JIGR1* synergistically interacts with *jing*-interactors in the adult eye

Results demonstrated that ectopic expression of JIGR1 and other *jing*-interactors in eye imaginal discs, using the glass-responsive GMR promoter, induced gene synthesis and loss of cells behind the morphenetic furrow. Furthermore, the extent of loss increased when *JIGR1* was co-expressed with *jing*-interactors, indicating possible genetic interactions between the genes.

The *gmr-GAL4* driver is commonly used for the mis-expression of transgenes in the developing eye. The GMR promoter is induced in third-instar eye-imaginal cells and the *glass* gene itself is required for normal photoreceptor cell development (Moses and Rubin, 1991). Each *jing*-interacting gene represents 1/600 EP lines tested in a GOF screen (Sun *et al.*, 2006). It was therefore important to examine the nature of these interactions in more detail at the cellular level. The four tested EP lines each showed a lack of secondary and tertiary pigment cells to varying degrees of disruption. In two lines, EP(3)3145 and EP(3)3354, mis-expression appeared to enhance the phenotypic effects where both R cells found within the ommatidium and the ommatidia array were displaced compared to the wildtype and *gmr-Gal4*-dependent expression of EP(3)635 and EP(3)3084. The development of the eye is possibly more sensitive to the gene dosage of the former two genes, one of which is *JIGR1*. This could be due to a direct consequence of up-regulation of these genes as they are required for proper eye differentiation and survival; or in an indirect manner where the up-regulation of these genes interfere with

other critical genes obligatory for development. Further analyses with loss-of-function phenotypes could provide valuable information.

There was an overall synergistic increase in phenotypic severity when *JIGR1* was co-expressed with each of the other three *jing*-interactors. All three combinations resulted in a complete lack of ommatidia and detectable pigment cells, resulting in a 'smooth' external morphology as examined by SEM. This could possibly signify not only a protein-protein interaction between the pairs but a combinatory effect as well. The molecular basis for these interactions is not clear, but there could be several possibilities. The first is that a genetic interaction may result from direct physical interaction between the two. More biochemical analyses are required to test this possibility. Another possibility is that JIGR1 and the other *jing*-interactors are part of a complex of regulators that work in parallel pathways that converge on the same end-point. This is difficult to test as there could be several hundred other genes under the same controls.

The replacement of ommatidia and other pigment cells by vacuoles could result from elimination by cellular apoptosis or from an interference with the initiation of neuronal cell determination or differentiation, or a combination of both. One method to test these ideas is by co-expressing the lines with a baculovirus p35 protein, an inhibitor of cell death (Hisahara *et al.*, 2000), and determining if there is any phenotypic suppression. A more direct approach is to stain the eye imaginal discs directly with acridine orange, a staining used to visualize nuclear changes and apoptotic body formation that are characteristic of apoptosis (Prins *et al.*, 1997). Cells are viewed under a fluorescence microscope where a fluorescent signal identifies an apoptotic cell.

In any event, the results establish that mis-expression of these four *jing*-interactors induces a rough eye phenotype through cell loss, and the severe disruption of eye development alludes to a genetic interaction between *JIGR1* with the other three *jing*-interactors.

Previous studies have been conducted by X. Sun (Sun *et al.*, 2006) for the characterization of another *jing*-interactor, EP(3)635 or *DATR-X* (also termed *dXNP*) has been characterized. Comparable to *JIGR1*, over-expression of *dXNP* in the developing eye under the control of *gmr-GAL4* destroyed all ommatidia. The similarities do not end there, co-expression of *DATR-X* with *jing*-interactors also resulted in more severe rough eye phenotypes including losses in pigmentation, representing synergistic interactions (Sun *et al.*, 2006). Acridine orange stainings of the eye provided direct evidence for *dXNP*-induced apoptosis of eye cells (Lee *et al.*, 2007). Moreover, it was found that over-expressed *dXNP* increases phosphorylation of Jun-N-terminal kinase (JNK) and the expression of direct targets of JNK pathway which plays a critical role in mediating apoptosis in the developing and mature organism (Donovan *et al.*, 2002;Lee *et al.*, 2007). These results demonstrate that dXNP regulates apoptosis directly via the JNK signalling pathway rather than regulation of the transcription of apoptotic factors. Therefore, should *JIGR1*-induced apoptosis of eye cells be confirmed, further tests of JIGR1's ability to regulates the JNK signaling pathway are required.

It has also been noted that *jing*-interactor, EP(3)3145, found upstream of *Drosophila ataxin2* (*Datx2*) was also found to interact with other *jing* enhancers but not with most randomly chosen EP lines (Sun *et al.*, 2006). Yet again, indicating these

specific EP lines belong to a unique group of genes that are functionally related pertaining to *jing* and to each other during eye development.

4.3 JIGR1 expression and subcellular localization

To help elucidate the function of JIGR1, we have examined the spatial and temporal distribution of its protein and mRNA through embryonic development. Using a rabbit polyclonal antibody against the product of the *JIGR1* gene, it was demonstrated that this protein is synthesized in the embryo at high levels during all stages of development, from the syncytial blastoderm embryo to the later, more specialized embryo right before entering its larval phases. Given its widespread distribution, it is very likely that *JIGR1* is an essential gene required for a basic cellular function. Many studies suggest that genes which are active at multiple stages of development are most likely indispensable (Mason *et al.*, 2003).

In younger embryos at the blastoderm and early gastrulation stages (Figure 11C and D) an abundant amount of JIGR1 was recognized by the antibody. This is expected as it is the period when transcription of all classes of genes is massively increased and the genome reaches its greatest transcriptional activity during embryogenesis (Yasuda *et al.*, 1991). In the blastula, it is likely that JIGR1 protein is translated from maternally inherited mRNA, before the embryo is able to transcribe its own embryonic genes, it is strictly dependent on stored maternal mRNA. Even as the embryo grows and zygotic control of development begins, there is transition from the synchronous, maternally controlled cycles to the asynchronous, zygotically controlled cycles (Yasuda *et al.*, 1991;Watson, 2007).

As the embryo enters gastrulation, JIGR1 protein is still present ubiquitously and generously. When magnified, JIGR1 appears to be localized in the nuclei at the subcellular level. Immunolocalization of JIGR1 in S2 cells further supported this observation and revealed that both full length JIGR1 and JIGR1ΔMADF were predominantly present in nuclei identified with DAPI (Figure 10). If JIGR1 were to have transcriptional regulatory function, JIGR1 is expected to be seen in the nucleus. The absence of any known nuclear localization signals (NLS) in the whole protein suggests that JIGR1 possibly accumulates in cell nuclei when initially synthesized and remain nuclear throughout embryogenesis. It is also possible that JIGR1 may dimerize with another protein containing a NLS, such as Jing (Sedaghat *et al.*, 2002), and be transported to the nucleus together. A small amount of protein was present in the cytoplasm in nearly all S2 cells transfected with JIGR1ΔMADF compared to the few observed in full length JIGR1 (Figure 10F). One possible explanation for this phenomenon is that since the truncated protein is roughly 1/3 shorter in length, it has a greater capacity to enter the cytoplasm by diffusing through the nuclear pore complex. Conversely, if JIGR1 were to bind to another protein in order to retain in the nucleus, a deletion may affect this bond and reduce nuclei localization.

In older embryos which are completing embryogenesis, JIGR1 expression was still ubiquitously distributed throughout the embryo, but higher levels of the protein now concentrate around defined structures (Figure 11F-H). Various fully differentiated systems could be identified from the same embryo at different focal planes. In Figure 11F and G, JIGR1 was clearly depicted in both the ectodermal cells and in the relatively more dorsally located ventral nerve cord (VNC). This correlates with the VNC pattern of

transcripts observed in embryos treated for *in situ* hybridization with a JIGR1 dig-labelled RNA probe (Figure 12F). The antibody was able to precisely distinguish the cells in and around the midline of the CNS. JIGR1 immunoreactivity was more pronounced in a group of cells visible in a segmentally repeated pattern in sagittal views of stage 14 embryos. Double labelling analyses have since shown that these structures are part of the PNS (Sonnenfeld, unpublished results). These results prompt the need for additional experiments of JIGR1 function during PNS development.

4.4 Essential functions of *JIGR1*

It has been established that loss- and gain-of-function *jing* is associated with defects in CNS axon and tracheal tubule patterning. In the CNS midline, *jing* is required for commissural and longitudinal axon formation and a loss of *jing* function affects dorsal trunk and visceral branch development (Sedaghat *et al.*, 2002). Due to previous genetic interactions found between *JIGR1* and other *jing*-interactors and JIGR1 expression localized in the CNS, it is possible that JIGR1 is involved in Jing CNS function. Since *jing* is also strongly implicated in the differentiation of tracheal cells, it is beneficial to study *JIGR1* effects in the tracheal system, despite the lack of protein expression in that region.

It appears that *JIGR1* is a critical gene that regulates both the embryonic development of the CNS in which it is expressed, and tracheal formation where it does not. Our data suggest that levels of JIGR1 must be precisely regulated during *Drosophila* development. Too much or too little is fatal. Both over-expression and loss of *JIGR1* mutants displayed disruption for patterning of axon structures and tracheal tubules with

the tested markers. These results are consistent with *jing* gain and loss-of-function phenotypes (Sedaghat *et al.*, 2002).

Over-expression of *JIGR1* in all CNS glial cells using the *gcm-Gal4* driver, resulted in developmental arrest of most major axon tracts that shape the CNS. The most common phenotype observed was a collapse of the segmental commissures. Longitudinal tracts were also affected to various extents of severity, including a slight thinning or a complete breakage of the axons. This demonstrates that *JIGR1* dose, like *jing*, is critical in CNS glial cells for their known role in axon guidance (Doe *et al.*, 1991).

In embryos double homozygously deficient for a segment of chromosome which includes *JIGR1*, similar mutations were observed as *JIGR1* amplified embryos. The loss of *JIGR1* function appears to generate a stronger disruption of the CNS, the commissures are even less defined and certain segments of longitudinal axons have completely severed. As with most *in vivo* studies it is difficult to assess and compare severity of defects between two samples, expressivity levels were measured to quantify the defects. Both gain and loss-of-function *JIGR1* retained very high levels of expressivity and the difference between not significant enough to conclude whether the additional or deletion of *JIGR1* produced more severe outcomes.

Embryos which were double heterozygous for both *jing* and deficiency covering *JIGR1* locus were examined using the same CNS markers. Once more, a similar phenotype appeared in terms of collapsed commissures and strained longitudinals. This once again supports the idea that *jing* is genetically related to a gene or genes in the cytogenetic region covered by *Def(3R)Exel6203*. If no genetic interactions existed, the expressivity level should be comparable those of controls (embryos heterozygous for

either *jing* or *Def(3R)Exel6203*) where no CNS defects occurred. However, an expressivity of over 50% was found in double heterozygotes. Therefore, *jing* is genetically interacting with *JIGR1* and/or other genes deleted by *Def(3R)Exel6203* to control CNS axon guidance.

Both over-expression *JIGR1* and homozygous *Def(3R)Exel6203* affected tubule formation in all tracheal lineages. In both cases, there were severe defects in dorsal trunk development and the complete lack of visceral branch differentiation. The defects in dorsal trunk and visceral branch formation are once again similar to the phenotypes observed in *jing* mutant embryos (Sedaghat *et al.*, 2002;Sonnenfeld *et al.*, 2004). Unlike in the CNS, where a possible genetic interaction between *jing* and *JIGR1* could exist according to the results seen in $jing^{3}$/*Def(3R)Exel 6203* heterozygous embryos, there does not appear to be a similar interaction in the trachea of these heterozygotes (results not shown). Nevertheless, *JIGR1* dosage still remains highly vital for proper tracheal formation.

Studies involving *in vitro* analysis of *JIGR1* interaction on the *btl* promoter, which is regulated by *jing in vivo* (Sonnenfeld in preparation), supported my *in vivo* findings. During luciferase assays, we concluded that *JIGR1* does not promote *btl* expression by directly interacting with the tracheal transcription complex, including Trh::Tgo heterodimers. In fact, it was statistically shown that contrary to previous presumptions, *jing* too, does not increase *btl* expression at this promoter region. Rather, it functions to bring about a decrease in transcription levels. Comparably, manipulations with *JIGR1* and co-expressing *JIGR1* and *jing* all demonstrated a similar outcome.

It is important to note that *in vitro* studies such as luciferase assays are not always an accurate reflection of *in vivo* conditions. There are many variables that are not controlled. Such as the possibility of S2 cells not compatible to receive *JIGR1* and *jing* insertions and created a competitive environment for *trh* and *tgo* to bind to the promoter, hence lowering the level of transcription. Direct *in vivo* experiments should be conducted to determine *JIGR1*'s effects on *btl*. A good way to evaluate effects is to perform *in situ* hybridizations in loss and gain-of-function *JIGR1* embryos with a *btl* RNA probe.

4.5 Future Directions

Up until now, our experiments are mainly based on gain-of-function procedures. Gain-of-function screenings are effective for causing dominant phenotypes and concluding that *JIGR1* is a dose sensitive gene. The loss-of-function line we have been using, *df(3R)Exel6203*, consists of gene deficiency at the cytogenetic region where *JIGR1* is found. Therefore, there could be a depletion of overlapping genes within this area and in turn, contributing to the observed genetic interactions. In order to precisely characterize *JIGR1* we need to generate loss-of-function *JIGR1* alleles.

One method is to produce JIGR1 RNAi lines. RNAi is a powerful tool for sequence-specific suppression. It utilizes the same principles as the UAS/GAL4 system and can direct the down-regulation of the gene both spatially and temporally. Seeing as RNAi can only serve to down-regulate JIGR1 expression and not eliminate it completely, a *JIGR1* mutant line is also required. Given that we already have the EP(3)3354 *JIGR1* line, we can take advantage of the *P* element transposon in the line to generate excision mutants (Gloor *et al.*, 2000). Unlike deficient lines, only a small proportion of DNA

around the original P element insertion point is deleted, minimizing chances of interfering with other genes.

Currently, the UAS-JIGR1 and UAS-JIGR1ΔMADF transgenic flies have been injected and are currently being expanded by a postdoctoral researcher in the Sonnenfeld lab. Once the lines are complete and functionally tested, we can attempt to rescue both loss-of-function embryos and JIGR1 mutants with these transgenic lines. Rescue results can be compared and could potentially provide direct physical evidence of MADF domain function under *in vivo* conditions.

REFRENCES

Bhaskar V, Courey AJ (2002). The MADF-BESS domain factor Dip3 potentiates synergistic activation by Dorsal and Twist. *Gene* 299(1-2):173-184.

Bilen J, Bonini NM (2005). Drosophila as a model for human neurodegenerative disease. *Annu Rev Genet* 39:153-171.

Blair SS (2003). Genetic mosaic techniques for studying Drosophila development. *Development* 130(21):5065-5072.

Brand AH, Perrimon N (1993). Targeted gene expression as a means of altering cell fates and generating dominant phenotypes. *Development* 118(2):401-415.

Brose K, Bland KS, Wang KH, Arnott D, Henzel W, Goodman CS *et al.* (1999). Slit proteins bind Robo receptors and have an evolutionarily conserved role in repulsive axon guidance. *Cell* 96(6):795-806.

Carmeliet P, Tessier-Lavigne M (2005). Common mechanisms of nerve and blood vessel wiring. *Nature* 436(7048):193-200.

Chan HY, Bonini NM (2000). Drosophila models of human neurodegenerative disease. *Cell Death Differ* 7(11):1075-1080.

Chiang C, Young KE, Beachy PA (1995). Control of Drosophila tracheal branching by the novel homeodomain gene unplugged, a regulatory target for genes of the bithorax complex. *Development* 121(11):3901-3912.

Crews ST (1998). Control of cell lineage-specific development and transcription by bHLH-PAS proteins. *Genes Dev* 12(5):607-620.

Crowther DC, Page R, Chandraratna D, Lomas DA (2006). A Drosophila model of Alzheimer's disease. *Methods Enzymol* 412:234-255.

Cummings JL, Cole G (2002). Alzheimer disease. *JAMA* 287(18):2335-2338.

Cutler G, Perry KM, Tjian R (1998). Adf-1 is a nonmodular transcription factor that contains a TAF-binding Myb-like motif. *Mol Cell Biol* 18(4):2252-2261.

Dickson BJ (2002). Molecular mechanisms of axon guidance. *Science* 298(5600):1959-1964.

Dickson BJ, Gilestro GF (2006). Regulation of commissural axon pathfinding by slit and its Robo receptors. *Annu Rev Cell Dev Biol* 22:651-675.

Dierick HA, Bejsovec A (1998). Functional analysis of Wingless reveals a link between intercellular ligand transport and dorsal-cell-specific signaling. *Development* 125(23):4729-4738.

Doe CQ, Chu-LaGraff Q, Wright DM, Scott MP (1991). The prospero gene specifies cell fates in the Drosophila central nervous system. *Cell* 65(3):451-464.

Doe CQ, Goodman CS (1985). Early events in insect neurogenesis. II. The role of cell interactions and cell lineage in the determination of neuronal precursor cells. *Dev Biol* 111(1):206-219.

Donovan N, Becker EB, Konishi Y, Bonni A (2002). JNK phosphorylation and activation of BAD couples the stress-activated signaling pathway to the cell death machinery. *J Biol Chem* 277(43):40944-40949.

Duffy JB (2002). GAL4 system in Drosophila: a fly geneticist's Swiss army knife. *Genesis* 34(1-2):1-15.

Egger B, Leemans R, Loop T, Kammermeier L, Fan Y, Radimerski T *et al.* (2002). Gliogenesis in Drosophila: genome-wide analysis of downstream genes of glial cells missing in the embryonic nervous system. *Development* 129(14):3295-3309.

England BP, Admon A, Tjian R (1992). Cloning of Drosophila transcription factor Adf-1 reveals homology to Myb oncoproteins. *Proc Natl Acad Sci U S A* 89(2):683-687.

Feany MB, Bender WW (2000). A Drosophila model of Parkinson's disease. *Nature* 404(6776):394-398.

Frankfort BJ, Mardon G (2002). R8 development in the Drosophila eye: a paradigm for neural selection and differentiation. *Development* 129(6):1295-1306.

Freeman MR, Delrow J, Kim J, Johnson E, Doe CQ (2003). Unwrapping glial biology: Gcm target genes regulating glial development, diversification, and function. *Neuron* 38(4):567-580.

Ghabrial A, Luschnig S, Metzstein MM, Krasnow MA (2003). Branching morphogenesis of the Drosophila tracheal system. *Annu Rev Cell Dev Biol* 19:623-647.

Gloor GB, Moretti J, Mouyal J, Keeler KJ (2000). Distinct P-element excision products in somatic and germline cells of Drosophila melanogaster. *Genetics* 155(4):1821-1830.

Goodman CS, Doe CQ (1993). Embryonic Development of the *Drosophila* Central Nervous System. In: The Development of *Drosophila melanogaster*. Bate M, Arias AM, editors. Cold Spring Harbor Laboratory Press, pp. 1131-1206.

Guillemin K, Groppe J, Ducker K, Treisman R, Hafen E, Affolter M *et al.* (1996). The pruned gene encodes the Drosophila serum response factor and regulates cytoplasmic outgrowth during terminal branching of the tracheal system. *Development* 122(5):1353-1362.

Gunawardena S, Goldstein LS (2001). Disruption of axonal transport and neuronal viability by amyloid precursor protein mutations in Drosophila. *Neuron* 32(3):389-401.

Han Z, Li X, Wu J, Olson EN (2004). A myocardin-related transcription factor regulates activity of serum response factor in Drosophila. *Proc Natl Acad Sci U S A* 101(34):12567-12572.

Hartenstein V (1993). Atlas of Drosophila Development. Cold Spring Harbor Laboratory Press.

Hay BA, Wolff T, Rubin GM (1994). Expression of baculovirus P35 prevents cell death in Drosophila. *Development* 120(8):2121-2129.

Hidalgo A, Urban J, Brand AH (1995). Targeted ablation of glia disrupts axon tract formation in the Drosophila CNS. *Development* 121(11):3703-3712.

Hiramoto M, Hiromi Y (2006). ROBO directs axon crossing of segmental boundaries by suppressing responsiveness to relocalized Netrin. *Nat Neurosci* 9(1):58-66.

Hisahara S, Araki T, Sugiyama F, Yagami K, Suzuki M, Abe K *et al.* (2000). Targeted expression of baculovirus p35 caspase inhibitor in oligodendrocytes protects mice against autoimmune-mediated demyelination. *EMBO J* 19(3):341-348.

Huber AB, Kolodkin AL, Ginty DD, Cloutier JF (2003). Signaling at the growth cone: ligand-receptor complexes and the control of axon growth and guidance. *Annu Rev Neurosci* 26:509-563.

Hummel T, Schimmelpfeng K, Klambt C (1999). Commissure formation in the embryonic CNS of Drosophila. *Dev Biol* 209(2):381-398.

Ikeda Y, Yamamoto J, Okamura M, Fujino T, Takahashi S, Takeuchi K *et al.* (2001). Transcriptional regulation of the murine acetyl-CoA synthetase 1 gene through multiple clustered binding sites for sterol regulatory element-binding proteins and a single neighboring site for Sp1. *J Biol Chem* 276(36):34259-34269.

Jacobs JR, Goodman CS (1989). Embryonic development of axon pathways in the Drosophila CNS. I. A glial scaffold appears before the first growth cones. *J Neurosci* 9(7):2402-2411.

Jacobs JR, Hiromi Y, Patel NH, Goodman CS (1989). Lineage, migration, and morphogenesis of longitudinal glia in the Drosophila CNS as revealed by a molecular lineage marker. *Neuron* 2(6):1625-1631.

Jarecki J, Johnson E, Krasnow MA (1999). Oxygen regulation of airway branching in Drosophila is mediated by branchless FGF. *Cell* 99(2):211-220.

Jazwinska A, Ribeiro C, Affolter M (2003). Epithelial tube morphogenesis during Drosophila tracheal development requires Piopio, a luminal ZP protein. *Nat Cell Biol* 5(10):895-901.

Keleman K, Rajagopalan S, Cleppien D, Teis D, Paiha K, Huber LA *et al.* (2002). Comm sorts robo to control axon guidance at the Drosophila midline. *Cell* 110(4):415-427.

Kidd T, Bland KS, Goodman CS (1999). Slit is the midline repellent for the robo receptor in Drosophila. *Cell* 96(6):785-794.

Kim J, Jones BW, Zock C, Chen Z, Wang H, Goodman CS *et al.* (1998). Isolation and characterization of mammalian homologs of the Drosophila gene glial cells missing. *Proc Natl Acad Sci U S A* 95(21):12364-12369.

Leal NA, Olteanu H, Banerjee R, Bobik TA (2004). Human ATP:Cob(I)alamin adenosyltransferase and its interaction with methionine synthase reductase. *J Biol Chem* 279(46):47536-47542.

Lee NG, Hong YK, Yu SY, Han SY, Geum D, Cho KS (2007). dXNP, a Drosophila homolog of XNP/ATRX, induces apoptosis via Jun-N-terminal kinase activation. *FEBS Lett* 581(14):2625-2632.

Leiserson WM, Benzer S, Bonini NM (1998). Dual functions of the Drosophila eyes absent gene in the eye and embryo. *Mech Dev* 73(2):193-202.

Liu Y, Montell DJ (2001). Jing: a downstream target of slbo required for developmental control of border cell migration. *Development* 128(3):321-330.

Ljunggren EL, Bergstrom K, Morrison DA, Mattsson JG (2006). Characterization of an atypical antigen from Sarcoptes scabiei containing an MADF domain. *Parasitology* 132(Pt 1):117-126.

Lloyd V, Ramaswami M, Kramer H (1998). Not just pretty eyes: Drosophila eye-colour mutations and lysosomal delivery. *Trends Cell Biol* 8(7):257-259.

Manev H, Dimitrijevic N, Dzitoyeva S (2003). Techniques: fruit flies as models for neuropharmacological research. *Trends Pharmacol Sci* 24(1):41-43.

Marlow SA, Wilson LE, Lawrie AM, Wilkinson N, King LA (1998). Assembly of Amsacta moorei entomopoxvirus spheroidin into spheroids following synthesis in insect cells using a baculovirus vector. *J Gen Virol* 79 (Pt 3):623-628.

Mason DA, Mathe E, Fleming RJ, Goldfarb DS (2003). The Drosophila melanogaster importin alpha3 locus encodes an essential gene required for the development of both larval and adult tissues. *Genetics* 165(4):1943-1958.

McGuire SE, Roman G, Davis RL (2004). Gene expression systems in Drosophila: a synthesis of time and space. *Trends Genet* 20(8):384-391.

Metzger RJ, Krasnow MA (1999). Genetic control of branching morphogenesis. *Science* 284(5420):1635-1639.

Moses K (2003). Drosophila Eye: Progressive Neural Development. Encyclopedia of Life Sciences. John Wiley & Sons, Ltd. http://mrw.interscience.wiley.com/ [10.1038/npg.els.0001147].

Moses K, Rubin GM (1991). Glass encodes a site-specific DNA-binding protein that is regulated in response to positional signals in the developing Drosophila eye. *Genes Dev* 5(4):583-593.

Nambu JR, Franks RG, Hu S, Crews ST (1990). The single-minded gene of Drosophila is required for the expression of genes important for the development of CNS midline cells. *Cell* 63(1):63-75.

Ohshiro T, Emori Y, Saigo K (2002). Ligand-dependent activation of breathless FGF receptor gene in Drosophila developing trachea. *Mech Dev* 114(1-2):3-11.

Ohshiro T, Saigo K (1997). Transcriptional regulation of breathless FGF receptor gene by binding of TRACHEALESS/dARNT heterodimers to three central midline elements in Drosophila developing trachea. *Development* 124(20):3975-3986.

Patel NH (1994). Imaging neuronal subsets and other cell types in whole-mount Drosophila embryos and larvae using antibody probes. *Methods Cell Biol* 44:445-487.

Pignoni F, Hu B, Zipursky SL (1997). Identification of genes required for Drosophila eye development using a phenotypic enhancer-trap. *Proc Natl Acad Sci U S A* 94(17):9220-9225.

Polymeropoulos MH, Lavedan C, Leroy E, Ide SE, Dehejia A, Dutra A *et al.* (1997). Mutation in the alpha-synuclein gene identified in families with Parkinson's disease. *Science* 276(5321):2045-2047.

Prins JB, Niesler CU, Winterford CM, Bright NA, Siddle K, O'Rahilly S *et al.* (1997). Tumor necrosis factor-alpha induces apoptosis of human adipose cells. *Diabetes* 46(12):1939-1944.

Reichman-Fried M, Shilo BZ (1995). Breathless, a Drosophila FGF receptor homolog, is required for the onset of tracheal cell migration and tracheole formation. *Mech Dev* 52(2-3):265-273.

Reiter LT, Potocki L, Chien S, Gribskov M, Bier E (2001). A systematic analysis of human disease-associated gene sequences in Drosophila melanogaster. *Genome Res* 11(6):1114-1125.

Richards S, Liu Y, Bettencourt BR, Hradecky P, Letovsky S, Nielsen R *et al.* (2005). Comparative genome sequencing of Drosophila pseudoobscura: chromosomal, gene, and cis-element evolution. *Genome Res* 15(1):1-18.

Rorth P (1996). A modular misexpression screen in Drosophila detecting tissue-specific phenotypes. *Proc Natl Acad Sci U S A* 93(22):12418-12422.

Rorth P (1998). Gal4 in the Drosophila female germline. *Mech Dev* 78(1-2):113-118.

Rorth P, Szabo K, Bailey A, Laverty T, Rehm J, Rubin GM *et al.* (1998). Systematic gain-of-function genetics in Drosophila. *Development* 125(6):1049-1057.

Rothberg JM, Jacobs JR, Goodman CS, rtavanis-Tsakonas S (1990). slit: an extracellular protein necessary for development of midline glia and commissural axon pathways contains both EGF and LRR domains. *Genes Dev* 4(12A):2169-2187.

Samakovlis C, Hacohen N, Manning G, Sutherland DC, Guillemin K, Krasnow MA (1996). Development of the Drosophila tracheal system occurs by a series of morphologically distinct but genetically coupled branching events. *Development* 122(5):1395-1407.

Sanchez-Soriano N, Tear G, Whitington P, Prokop A (2007). Drosophila as a genetic and cellular model for studies on axonal growth. *Neural Develop* 2:9.

Sang TK, Jackson GR (2005). Drosophila models of neurodegenerative disease. *NeuroRx* 2(3):438-446.

Schneider I (1972). Cell lines derived from late embryonic stages of Drosophila melanogaster. *J Embryol Exp Morphol* 27(2):353-365.

Sedaghat Y, Miranda WF, Sonnenfeld MJ (2002). The jing Zn-finger transcription factor is a mediator of cellular differentiation in the Drosophila CNS midline and trachea. *Development* 129(11):2591-2606.

Sedaghat Y, Sonnenfeld M (2002). The jing gene is required for embryonic brain development in Drosophila [corrected]. *Dev Genes Evol* 212(6):277-287.

Shulman JM, Shulman LM, Weiner WJ, Feany MB (2003). From fruit fly to bedside: translating lessons from Drosophila models of neurodegenerative disease. *Curr Opin Neurol* 16(4):443-449.

Smith DB, Johnson KS (1988). Single-step purification of polypeptides expressed in Escherichia coli as fusions with glutathione S-transferase. *Gene* 67(1):31-40.

Sonnenfeld M, Ward M, Nystrom G, Mosher J, Stahl S, Crews S (1997). The Drosophila tango gene encodes a bHLH-PAS protein that is orthologous to mammalian Arnt and controls CNS midline and tracheal development. *Development* 124(22):4571-4582.

Sonnenfeld MJ, Barazesh N, Sedaghat Y, Fan C (2004). The jing and ras1 pathways are functionally related during CNS midline and tracheal development. *Mech Dev* 121(12):1531-1547.

Sonnenfeld MJ, Delvecchio C, Sun X (2005). Analysis of the transcriptional activation domain of the Drosophila tango bHLH-PAS transcription factor. *Dev Genes Evol* 215(5):221-229.

Spradling AC, Stern DM, Kiss I, Roote J, Laverty T, Rubin GM (1995). Gene disruptions using P transposable elements: an integral component of the Drosophila genome project. *Proc Natl Acad Sci U S A* 92(24):10824-10830.

Stevison LS, Counterman BA, Noor MA (2004). Molecular evolution of X-linked accessory gland proteins in Drosophila pseudoobscura. *J Hered* 95(2):114-118.

Strutt DI, Mlodzik M (1995). Ommatidial polarity in the Drosophila eye is determined by the direction of furrow progression and local interactions. *Development* 121(12):4247-4256.

Sun X, Morozova T, Sonnenfeld M (2006). Glial and neuronal functions of the Drosophila homolog of the human SWI/SNF gene ATR-X (DATR-X) and the jing zinc-finger gene specify the lateral positioning of longitudinal glia and axons. *Genetics* 173(3):1397-1415.

Sutherland D, Samakovlis C, Krasnow MA (1996). branchless encodes a Drosophila FGF homolog that controls tracheal cell migration and the pattern of branching. *Cell* 87(6):1091-1101.

Tear G, Harris R, Sutaria S, Kilomanski K, Goodman CS, Seeger MA (1996). commissureless controls growth cone guidance across the CNS midline in Drosophila and encodes a novel membrane protein. *Neuron* 16(3):501-514.

Tessier-Lavigne M, Placzek M, Lumsden AG, Dodd J, Jessell TM (1988). Chemotropic guidance of developing axons in the mammalian central nervous system. *Nature* 336(6201):775-778.

Uhler J, Garbern J, Yang L, Kamholz J, Mellerick DM (2002). Nk6, a novel Drosophila homeobox gene regulated by vnd. *Mech Dev* 116(1-2):105-116.

Volles MJ, Lansbury PT, Jr. (2003). Zeroing in on the pathogenic form of alpha-synuclein and its mechanism of neurotoxicity in Parkinson's disease. *Biochemistry* 42(26):7871-7878.

Wappner P, Gabay L, Shilo BZ (1997). Interactions between the EGF receptor and DPP pathways establish distinct cell fates in the tracheal placodes. *Development* 124(22):4707-4716.

Warren WD, Steffensen S, Lin E, Coelho P, Loupart M, Cobbe N *et al.* (2000). The Drosophila RAD21 cohesin persists at the centromere region in mitosis. *Curr Biol* 10(22):1463-1466.

Watson AJ (2007). Oocyte cytoplasmic maturation: a key mediator of oocyte and embryo developmental competence. *J Anim Sci* 85(13 Suppl):E1-E3.

Whitworth AJ, Wes PD, Pallanck LJ (2006). Drosophila models pioneer a new approach to drug discovery for Parkinson's disease. *Drug Discov Today* 11(3-4):119-126.

Yasuda GK, Baker J, Schubiger G (1991). Temporal regulation of gene expression in the blastoderm Drosophila embryo. *Genes Dev* 5(10):1800-1812.

Zimmermann G, Furlong EE, Suyama K, Scott MP (2006). Mes2, a MADF-containing transcription factor essential for Drosophila development. *Dev Dyn* 235(12):3387-3395.